Development 140, 3095-3106 (2013) doi:10.1242/dev.093716

ERF and ETV3L are retinoic acid-inducible repressors required for primary neurogenesis

Amanda Janesick[1], Rachelle Abbey[1], Connie Chung[1], Sophia Liu[1], Mao Taketani[1,*] and Bruce Blumberg[1,2,‡]

SUMMARY

Cells in the developing neural tissue demonstrate an exquisite balance between proliferation and differentiation. Retinoic acid (RA) is required for neuronal differentiation by promoting expression of proneural and neurogenic genes. We show that RA acts early in the neurogenic pathway by inhibiting expression of neural progenitor markers *Geminin* and *Foxd4l1*, thereby promoting differentiation. Our screen for RA target genes in early *Xenopus* development identified *Ets2 Repressor Factor* (*Erf*) and the closely related ETS repressors *Etv3* and *Etv3-like* (*Etv3l*). *Erf* and *Etv3l* are RA responsive and inhibit the action of ETS genes downstream of FGF signaling, placing them at the intersection of RA and growth factor signaling. We hypothesized that RA regulates primary neurogenesis by inducing *Erf* and *Etv3l* to antagonize proliferative signals. Loss-of-function analysis showed that *Erf* and *Etv3l* are required to inhibit proliferation of neural progenitors to allow differentiation, whereas overexpression of *Erf* led to an increase in the number of primary neurons. Therefore, these RA-induced ETS repressors are key components of the proliferation-differentiation switch during primary neurogenesis *in vivo*.

KEY WORDS: Differentiation, Ets repressors, Neural progenitor, Primary neurogenesis, Proliferation, Retinoic acid, *Xenopus*

INTRODUCTION

Primary neurogenesis is a phenomenon associated with anamniote embryos wherein sensorimotor neurons, which are largely transitory in nature, arise from neural-competent tissue and enable the early development of swimming and feeding behaviors (Wullimann et al., 2005). Primary neurogenesis is preceded by neural induction, which requires inhibition of bone morphogenetic protein (BMP) signaling (Wills et al., 2010; Wilson and Hemmati-Brivanlou, 1995) together with active fibroblast growth factor (FGF) signaling (reviewed by Dorey and Amaya, 2010; Marchal et al., 2009; Wills et al., 2010). Neural induction leads to the expression of pro-proliferative and neural-fate stabilizing transcription factors such as *Foxd4l1*, *Geminin*, *Sox2/3* and Zic-family genes (Branney et al., 2009; Marchal et al., 2009; Yan et al., 2009). The concerted action of these genes promotes proliferation and maintenance of immature neural precursors. Through an incompletely understood mechanism, neural progenitors of the deep neuroectoderm layer of the embryo exit from the cell cycle and differentiate into primary neurons (Chalmers et al., 2002) under the control of proneural and neurogenic transcription factors (reviewed by Rogers et al., 2009).

Retinoic acid (RA) has numerous effects on early development, mostly by acting as a differentiation agent and specifier of position along the body axes (reviewed by Maden, 2007; Niederreither and Dollé, 2008; Rhinn and Dollé, 2012). RA signaling is required for neuronal differentiation (Blumberg et al., 1997; Sharpe and Goldstone, 2000; Sharpe and Goldstone, 1997), inhibiting the expression of pro-proliferation genes while promoting expression of proneural and neurogenic genes (Franco et al., 1999). RA regulates the timing (Papalopulu and Kintner, 1996) and extent (Blumberg et al., 1997; Franco et al., 1999; Sharpe and Goldstone, 1997) of neuronal differentiation, but little is known about underlying molecular mechanisms.

One clue to how RA may be promoting neuronal differentiation came from cell culture systems where RA was shown to regulate expression of genes that facilitate cell cycle exit and differentiation, particularly in cancers (reviewed by Andrews, 1984; Gudas, 1992). FGF and mitogen-activated protein kinase (MAPK) signaling are pro-proliferative, whereas RA inhibits proliferation and promotes differentiation. FGF8 and RA signaling pathways oppose each other's action in patterning the anteroposterior (A-P) and dorsoventral (D-V), axes and in the differentiation of neurons and somites (Diez del Corral and Storey, 2004; Duester, 2008; Moreno and Kintner, 2004). How RA regulates the molecular components of the FGF signaling pathway to encourage differentiation is poorly understood.

ETS proteins comprise a family of transcription factors targeted by extracellular signaling pathways and modified by MAPK signaling downstream of growth factor receptors, integrins or Ca^{+2}/calmodulin-dependent protein kinases (Oikawa and Yamada, 2003; Sharrocks, 2001). ETS proteins can function as transcriptional activators or repressors that interact with other factors to facilitate combinatorial, context-specific regulation of gene expression (reviewed by Hollenhorst et al., 2011; Li et al., 2000; Mavrothalassitis and Ghysdael, 2000; Oikawa and Yamada, 2003; Sharrocks, 2001).

ETS proteins are implicated in early development of the central nervous system, eye and blood, and regulate cell growth, differentiation and apoptosis (reviewed by Hollenhorst et al., 2011; Oikawa and Yamada, 2003; Sharrocks, 2001). ETS repressors ERF (ETS2 Repressor Factor), ETV3 (ETS Variant Protein 3) and ETV3L (ETV3-like) are closely related genes (Hollenhorst et al., 2011; Laudet et al., 1999) that can regulate the switch between proliferation and differentiation in some cell types (Hester et al., 2007; Klappacher et al., 2002; Verykokakis et al., 2007). ERF and

[1]Department of Developmental and Cell Biology, 2011 Biological Sciences 3, University of California, Irvine, CA 92697-2300, USA. [2]Department of Pharmaceutical Sciences, University of California, Irvine, CA 92697-2300, USA.

*Present address: Department of Bioengineering and Therapeutic Sciences, University of California San Francisco, CA 94158, USA
‡Author for correspondence (blumberg@uci.edu)

Accepted 30 May 2013

ETV3 may displace activating ETS proteins from promoters of cell cycle control genes, while recruiting co-repressor complexes to facilitate cell cycle arrest. ERF and ETV3 are phosphorylated by ERK, which renders them inactive (Carlson et al., 2011; Hester et al., 2007). Phosphorylation of ERF leads to its nuclear export, whereas phosphorylation of ETV3 inhibits its DNA binding (Carlson et al., 2011; Hester et al., 2007). *Etv3* promotes cell cycle arrest and differentiation of macrophage progenitors (Klappacher et al., 2002). *Erf* inhibits proliferation of trophoblast stem cells, and encourages the differentiation of the chorion layer into the labyrinth in the extra-embryonic ectoderm (Papadaki et al., 2007). Thus, ETS repressors are ideal candidates for regulating a proliferation-differentiation switch in primary neurogenesis.

We have previously shown that some *Ets* genes were responsive to changes in RAR signaling in *Xenopus* embryos (Arima et al., 2005). *Erf* was upregulated by increased RA signaling in neurula embryos (Arima et al., 2005). Here, we show that morpholino oligonucleotide (MO)-mediated knockdown of *Erf* or *Etv3* results in loss of primary neurons accompanied by paralysis, phenocopying RAR loss of function. *Erf*, *Etv3/3l*, *Rarα* and *Rarγ* inhibit early neural progenitor markers, while promoting differentiation of primary neurons. Loss of any of these gene products results in a paucity of primary neurons in the neurula and renders tadpole-stage embryos unresponsive to touch. This loss of neurons is due to increased proliferation in the neural plate and a perpetuation of neural progenitor identity, at the expense of differentiation. *Erf* and *Etv3l* are thus key effectors of the RA-mediated switch between proliferation and differentiation during primary neurogenesis.

MATERIALS AND METHODS

Embryos

Xenopus eggs were fertilized *in vitro* (Janesick et al., 2012) and embryos staged according to Nieuwkoop and Faber (Nieuwkoop and Faber, 1967). Embryos were maintained in 0.1×MBS until appropriate stages or treated at stages 7/8 with 1 μM agonist (TTNPB) and 1 μM antagonist (AGN193109) as described previously (Janesick et al., 2012). Embryos were injected bilaterally or unilaterally at the two- or four-cell stage with combinations of gene specific morpholinos (MO), mRNA and 100 pg/embryo *β-galactosidase* (*β-gal*) mRNA or 10 ng/embryo 10 kDa lysine-fixable rhodamine-dextran lineage tracer. MO sequences are listed in supplementary material Table S1. For all MO experiments, control embryos were injected with 10 ng standard control MO (GeneTools).

Embryos processed for whole-mount *in situ* hybridization were fixed in MEMFA, stained for β-GAL activity with magenta-GAL (Biosynth) and then stored in 100% ethanol (Janesick et al., 2012). For whole-mount immunohistochemistry, embryos were fixed in MEMFA for 1 hour, permeabilized in Dent's Fixative (80% methanol, 20% DMSO) overnight and stored in 100% methanol.

Whole-mount *in situ* hybridization (WISH)

Whole-mount *in situ* hybridization was performed as previously described (Janesick et al., 2012; Koide et al., 2001; Sive et al., 1998). *Geminin*, *Foxd4l1*, *Neogenin*, *Sox3*, *Zic1* and *Zic3* probes were prepared via PCR amplification of published coding regions from cDNA, adding a bacteriophage T7 promoter to the 3′ end: *xGeminin* (Kroll et al., 1998; McGarry and Kirschner, 1998), *xFoxd4l1* (Sölter et al., 1999; Sullivan et al., 2001), *xNeogenin* (Anderson and Holt, 2002), *xSox3* (Denny et al., 1992; Penzel et al., 1997), *xZic1* (Kuo et al., 1998; Mizuseki et al., 1998; Nakata et al., 1998) and *xZic3* (Nakata et al., 1997). *Erf*- and *Etv3*-coding sequences (Klein et al., 2002) were cloned into pBluescript II SK–. Probes were transcribed with MEGAscript T7 (Ambion) in the presence of digoxigenin-11-UTP as described previously (Janesick et al., 2012). A list of forward primers and reverse primers containing a T7 promoter can be found in supplementary material Table S2. *N-tubulin* was a gift from Dr Nancy Papalopulu (University of Manchester, UK). *Zic2*, *Ngnr1*, *Myt1* and *Dl1* were a kind gift of Dr Andrés Carrasco (University of Buenos Aires, Argentina) (supplementary material Table S3).

N-tubulin expression was quantitated using Adobe Photoshop and ImageJ. Bright-field images were desaturated of magenta to remove lineage tracer signal. Purple whole-mount in situ hybridization signal was replaced with black and the images converted to binary and cropped such that the injected and uninjected sides were equal in total area. ImageJ was used to quantitate the black pixels as % area fraction using the Analyze → Measure function. The area fractions obtained for each side were normalized to the total area for each embryo. Statistical significance was determined using the Wilcoxon signed rank test in GraphPad Prism v5.0 (GraphPad Software, San Diego, CA). $P \leq 0.05$ was considered statistically significant.

Whole-mount immunohistochemistry

Embryos were photographed for fluorescence, then processed separately in individual wells of 96-well plates for whole-mount immunohistochemistry. Embryos were rehydrated in PBS, 0.5% Tween-20 and heated overnight at 65°C with shaking (Lin et al., 2012). After blocking in 2% blocking reagent (Roche), 10% FBS in MAB for 1 hour, embryos were incubated in a 1:1000 dilution of anti-phospho-histone 3 (Cat# 06-570, Millipore) or anti-PCNA (SC-7907, Santa Cruz Biotechnology) in blocking buffer at room temperature for 4 hours. Embryos were washed five times for 1 hour in MABT at 4°C, then blocked in 2% blocking reagent (Roche), 10% goat serum in MAB for 1 hour. AP-conjugated anti-rabbit IgG (Cat# A-3687, Sigma) was diluted 1:10,000 in blocking buffer and embryos incubated at room temperature for 4 hours. After five 1-hour MABT washes, BM purple staining followed by bleaching was performed according to standard methods (Janesick et al., 2012).

Embryos were photographed at 25× magnification in bright-field, with anterior always pointing left. Ovals were selected from each side of the neural plate, then desaturated and converted to binary in MATLAB. Phospho-*Histone H3*-positive or PCNA-positive staining was quantitated in MATLAB. Statistical significance was determined using the Wilcoxon signed rank test in MATLAB. $P \leq 0.05$ was considered statistically significant.

Transfection

Transient transfections were performed in COS-7 cells as described previously (Chamorro-García et al., 2012). Briefly, COS-7 cells were seeded at 1.8×10^4 cells/well in BD BioCoat poly-D-lysine eight-well culture slides in 10% CBS. Cells were transfected in Opti-MEM at ~90% confluency. pCS2-*mCherry* transfection control plasmid (0.25 μg/well) was co-transfected with 0.25 μg/well of pCDG1-FLAG-hGR-*Erf* plasmids (or minus-FLAG control) using Lipofectamine 2000 reagent (Invitrogen). After overnight incubation, the medium was replaced with DMEM/10% resin charcoal-stripped FBS (Tabb et al., 2004) plus 1 μM dexamethasone (DEX) or 0.01% DMSO vehicle for 1 hour before fixing cells in 10% formalin in PBS.

Immunofluorescence

Fixed, transfected COS-7 cells were washed with PBS, then permeabilized with 0.25% Triton X-100 in PBS for 10 minutes. Cells were incubated at room temperature with 5% goat serum in PBS for 1 hour to block nonspecific antibody binding, and then incubated for 1 hour with anti-FLAG-M2 (1:50, Sigma). Cells were washed with PBS and then incubated at room temperature with goat anti-mouse Alexa Fluor 488 (1:500, Invitrogen) in 5% goat serum for 1 hour. To visualize nuclei, cells were stained with 1 μg/ml Hoechst 33342 (Invitrogen) for 10 minutes. Fluorescent microscopy images were acquired with Velocity software on a Zeiss Axioplan 2 fluorescence microscope equipped with an ORCA-ER CCD camera (Hamamatsu Photonics). Images were merged with Adobe Photoshop. Images shown are representative of transfected (mCHERRY+) cells observed in each experiment.

QPCR

Total embryo RNA was DNase treated, LiCl precipitated and reverse transcribed into cDNA as described previously (Janesick et al., 2012). First-strand cDNA was quantitated using SYBR green detection (Roche) in a DNA Engine Opticon Continuous Fluorescence Detection System (Bio-

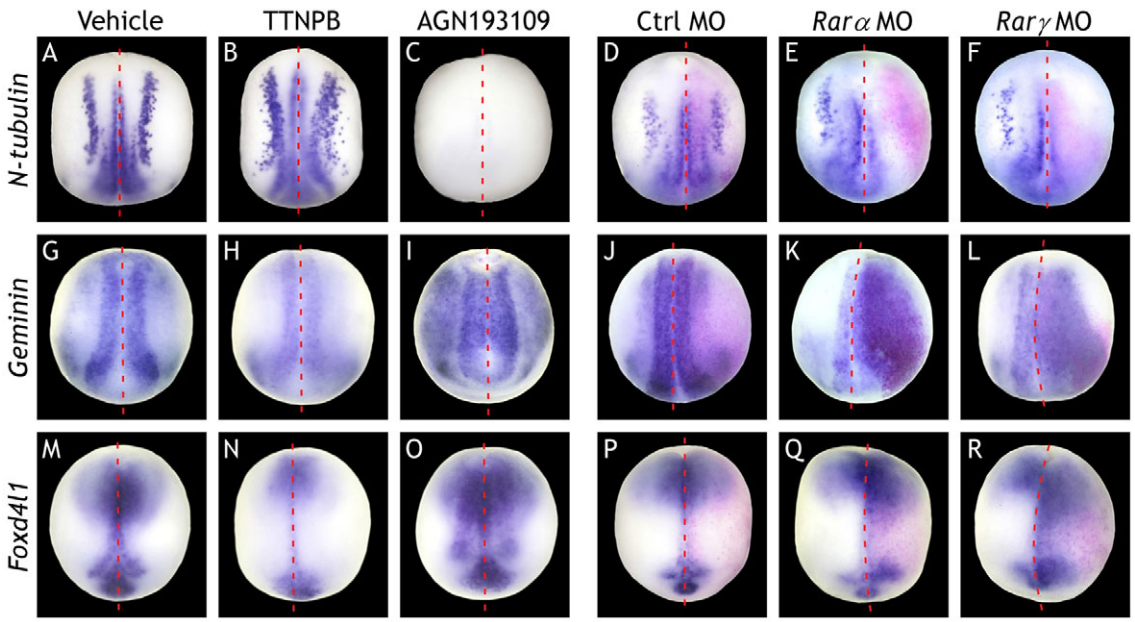

Fig. 1. *N-tubulin* is RA responsive, and requires RARα and RARγ for its expression; neural progenitor markers *Geminin* and *Foxd4l1* are modulated by RAR signaling. (A-C,G-I,M-O) Whole-mount *in situ* hybridization of *N-tubulin* expression from whole embryos treated at stage 7/8 with 1 μM TTNPB (an RAR-specific agonist), 1 μM AGN193109 (an RAR-specific antagonist) or control vehicle (0.1% ethanol). (**A**,**G**,**M**) Control expression of *N-Tubulin*, *Geminin* and *Foxd4l1*. (**B**,**C**) Overexpression of neurons was observed in 15/19 of TTNPB-treated embryos (B); loss of neurons was observed in 19/19 of AGN193109-treated embryos (C). (**H**,**N**) *Geminin* (9/9 embryos) and *Foxd4l1* (9/10) expression was diminished with TTNPB. (**I**,**O**) AGN193109 expanded *Geminin* (9/9) and *Foxd4l1* (14/14). (D-F,J-L,P-R) All embryos were injected unilaterally at the two- or four-cell stage. The injected side is indicated by the magenta *β-gal* mRNA lineage tracer. (**D**,**J**,**P**) Control expression of *N-tubulin, Geminin* and *Foxd4l1*. (**E**,**K**,**Q**) 3.3 ng *Rara1* MO + 3.3 ng *Rara2.1* MO + 3.3 ng *Rara2.2* MO reduced expression of *N-tubulin* (18/23 embryos), but expanded expression of *Geminin* (13/13) and *Foxd4l1* (14/20). (**F**,**L**,**R**) 3.75 ng *Rarγ1* MO + 3.75 *Rarγ2* MO reduced expression of *N-tubulin* (34/34), but expanded expression of *Geminin* (35/35) and *Foxd4l1* (14/16). Embryos are shown in dorsal view at stage 14; anterior is at the bottom.

Rad) using primer sets listed in supplementary material Table S4. Each primer set amplified a single band, as determined by gel electrophoresis and melting curve analysis. In Fig. 2A, QPCR data were analyzed using the ΔΔCt method (Livak and Schmittgen, 2001) normalizing to *Histone H4* (Janesick et al., 2012). Mann-Whitney statistical analysis was performed in GraphPad Prism v5.0. For Fig. 3L, QPCR data was analyzed by ΔCt normalizing to *Histone H4*, and correcting for amplification efficiency between *Erf*, *Etv3* and *Etv3l* (Pfaffl, 2001). Error bars in Fig. 2A, Fig. 3L and supplementary material Fig. S2 represent biological replicates (multiple pools of five embryos from the same female) calculated using standard propagation of error.

Cloning of pCDG1-FLAG-hGR-Erf constructs

The *Erf* expression construct was made by PCR amplification of the protein-coding regions of the *Erf* cDNA and cloned into pCDG1 (Janesick et al., 2012). pCDG1-*hGR-Erf* was constructed by two-fragment PCR using pCDG1-*Erf* and amino acid residues 512-777 of the *hGR* (provided by Ron Evans, Salk Institute, San Diego, CA, USA) as templates, and cloned into pCDG1 (supplementary material Table S5). *hGR-Erf* ($Ser^{246,251}$ → $Ala^{246,251}$) and *hGR-Erf* ($Ser^{246,251}$ → $Glu^{246,251}$) were also constructed by two-fragment PCR and cloned into pCDG1 (supplementary material Table S6). Plasmids were sequence verified and linearized with *Not*I; mRNA was transcribed using mMessage mMachine T7 (Ambion).

RESULTS

RAR signaling induces neuronal differentiation and inhibits pro-proliferative neural markers

RA signaling is required for neuronal differentiation (Blumberg et al., 1997; Sharpe and Goldstone, 2000; Sharpe and Goldstone, 1997), inhibiting the expression of anti-neurogenic genes (e.g. *Zic2*) while promoting expression of proneural and neurogenic genes (Franco et al., 1999). As little is known about the underlying molecular mechanisms, we investigated how RA and its nuclear receptors promote primary neurogenesis.

Rarα and *Rarγ* are localized in the neural plate at stage 14, the correct time and place to regulate primary neurogenesis (supplementary material Fig. S1A,B) (Sharpe, 1992). Overexpression of *Rxrβ* and *Rarα2* produced ectopic neurons, whereas dominant negative *Rarα1* or *Rarα2* resulted in loss of primary neurons (Blumberg et al., 1997; Sharpe and Goldstone, 1997). Treatment of embryos with the RAR-specific agonist, TTNPB, increased primary neuron formation within the neural plate (Fig. 1B); treatment with the RAR-specific antagonist AGN193109 led to the loss of neurons (Fig. 1C) and subsequent paralysis (embryos did not spontaneously move and were unresponsive to touch). This agrees with previous results using less specific chemicals, including RA, Ro 41-5253 and citral (Franco et al., 1999; Sharpe and Goldstone, 2000). Effects on neurogenesis were observed at 10^{-9} M for TTNPB and at 10^{-7} M for AGN193109 (supplementary material Fig. S2A,B). The direct RAR target gene *HoxA1* (Balmer and Blomhoff, 2002; Sive and Cheng, 1991) was significantly upregulated by TTNPB and downregulated by AGN193109 at 10^{-8} M (supplementary material Fig. S2C). This demonstrates that the *N-tubulin* phenotypes at 10^{-6} M TTNPB or 10^{-6} M AGN193109 are not off-target non-specific effects.

Published data do not distinguish whether RARα, RARγ or both are required for primary neurogenesis. Using MO-mediated gene knockdown, we found that microinjection of either an *Rarα* MO (Fig. 1E) or an *Rarγ* MO (Fig. 1F) greatly diminished the number of primary neurons (revealed by *N-tubulin* expression) compared

with control MO (Fig. 1D). Phenotypes were verified by reproducing them with different MOs (supplementary material Fig. S3). The sequences targeted by each MO show no similarity to each other (supplementary material Fig. S4). We infer that primary neurogenesis requires both RARα and RARγ; therefore, these receptors are not functionally redundant. Loss of the RA metabolizing enzymes RALDH2 or CYP26A1 caused the expected loss or gain of primary neurons, respectively (supplementary material Fig. S5). The phenotypes are weaker and less penetrant than those elicited by the *Rar* MOs, suggesting that these enzymes are not exclusively responsible for the steady state of RA within the embryo or, alternatively, that eliminating enzymatic activity may require more complete knockdown than could be achieved.

RAR was predicted to be involved in the pre-patterning stage of neurogenesis, with less pivotal roles during earlier stages of neural induction or the later process of lateral inhibition because treatment with RA inhibited expression of *Zic2* (Franco et al., 1999), a pre-patterning gene that inhibits differentiation of neural precursors wherever it is expressed (Brewster et al., 1998). To address where RA signaling acts during neurogenesis, we asked whether modulating RAR signaling altered expression of *Geminin*, *Foxd4l1* (also known as *FoxD5*) and *Sox3*, all early markers of neural progenitors whose overexpression inhibits differentiation. TTNPB treatment decreased the sizes of *Geminin* (Fig. 1H) and *Foxd4l1* (Fig. 1N) expression domains compared with controls (Fig. 1G,M), whereas it had little effect on *Sox3* (supplementary material Fig. S6A,B). Treatment with AGN193109 markedly expanded *Geminin* (Fig. 1I), *Foxd4l1* (Fig. 1O) and *Sox3* expression domains, particularly in the anterior (supplementary material Fig. S6C). Knockdown of either *Rarα* or *Rarγ* expanded the *Geminin* (Fig. 1K,L), *Foxd4l1* (Fig. 1Q,R) and *Sox3* expression domains (supplementary material Fig. S6E,F); the control MO had no effect (Fig. 1J,P; supplementary material Fig. S6D). These results indicated that RAR activation decreased the expression of early markers, whereas inhibition of RAR action expanded the expression domains.

Erf and Etv3l are RAR-responsive ETS repressors expressed in the neuroectoderm

As RA signaling is required for primary neurogenesis, we asked which genes might mediate the effects of RA on neuronal differentiation. Our previous microarray analysis revealed that *Ets2 Repressor Factor* (*Erf*) was upregulated by TTNPB at neurula stages (Arima et al., 2005). *Erf* is closely related to two other ETS repressors, *Ets Variant 3* (*Etv3*) and *Etv3-like*, which are linked in mammalian and *Xenopus* genomes (Hellsten et al., 2010; Muffato et al., 2010). *Erf* and *Etv3* negatively regulate the cell cycle to inhibit proliferation by interfering with the function of ETS activators (e.g. *Ets1/2*) at the transcriptional level. Initial experiments showed that MO-mediated knockdown of *Etv3/3l* or *Erf* rendered microinjected *Xenopus* embryos unresponsive to touch (not shown), similar to RAR loss of function (Blumberg et al., 1997). We hypothesized that *Erf* and *Etv3/3l* might be important downstream effectors of RA action in primary neurogenesis.

Quantitative real time RT-PCR (QPCR) analysis showed that *Erf* and *Etv3l* are RA-responsive at the early neurula stage (Fig. 2A). *Erf* was more strongly induced by RA during early and late neurula stages, compared with *Etv3* and *Etv3l* (Fig. 2A). Whole-mount *in situ* hybridization revealed that *Erf* expression was expanded in TTNPB-treated embryos (Fig. 2C): the normally sharp expression of *Erf* in the neural folds was broadened and was ectopically present in the anterior. Erf expression was blurred by AGN193109

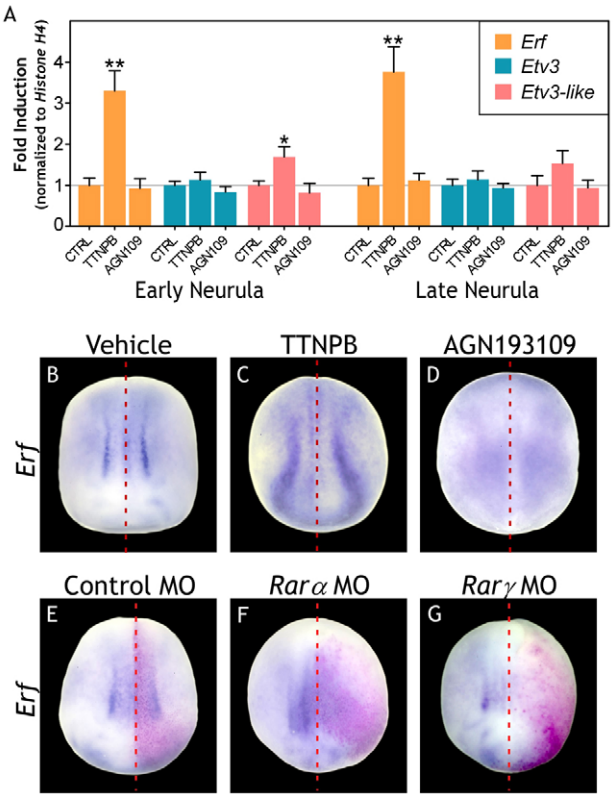

Fig. 2. RAR signaling modulates *Erf* and *Etv3l* expression. (**A**) QPCR showing *Erf*, *Etv3* and *Etv3l* expression in embryos treated at stage 7/8 with 1 μM TTNPB, 1 μM AGN193109 or vehicle (0.1% ethanol). The *y*-axis represents $2^{-\Delta\Delta Ct}$ values normalized to *Histone H4* and expressed as fold induction relative to control. *Erf* is induced by TTNPB, *Etv3l* is induced by TTNPB in early neurula, whereas *Etv3* is not. Asterisks represent statistical significance compared with control (*=$P \leq 0.05$, **=$P \leq 0.01$). (**B-D**) Whole-mount *in situ* hybridization of *Erf* expression from whole embryos treated at stage 7/8 with 1 μM TTNPB, 1 μM AGN193109 or vehicle (0.1% ethanol). Expansion of *Erf* was observed in 13/13 of TTNPB-treated embryos; blurring of *Erf* expression in the neural folds was observed in 13/13 of AGN193109-treated embryos. (**E-G**) Embryos were injected unilaterally at the two- or four-cell stage. The injected side is indicated by the magenta lineage tracer. (E) Control expression of *Erf*. (F) 3.3 ng *Rara1* MO + 3.3 ng *Rara2.1* MO + 3.3 ng *Rara2.2* MO reduced expression of *Erf* (10/10). (G) 3.75 ng *Rarγ1* MO + 3.75 *Rarγ2* MO reduced expression of *Erf* (11/11). Embryos are shown in dorsal view at stage 14; anterior is at the bottom.

(Fig. 2D), and knockdown of RARα (Fig. 2F) and RARγ (Fig. 2G). *Etv3/Etv3l* are ubiquitously expressed in the neurula (see below) and expression was not altered detectably by whole-mount *in situ* hybridization. These results support a role for *Erf* and *Etv3l* as potential downstream effectors of RA signaling in primary neurogenesis.

We used whole-mount *in situ* hybridization to determine whether *Erf* and *Etv3/3l* were expressed appropriately to act downstream of RA signaling in primary neurogenesis (Fig. 3). Prior to gastrulation, *Etv3/3l* (not shown) and *Erf* (Fig. 3A,B) are present in the animal, but absent from the vegetal hemisphere. At the open neural plate stage, *Etv3/3l* expression is broad and diffuse in the neural plate (supplementary material Fig. S1D) but absent from the ventral side of the embryo. *Erf* is expressed throughout the neural plate by stage 13, and concentrated in the neural folds (Fig. 3C-F; supplementary material Fig. S1C). *Erf* expression later becomes pronounced in the head, particularly the eye, otocyst, forebrain and pharyngeal arches,

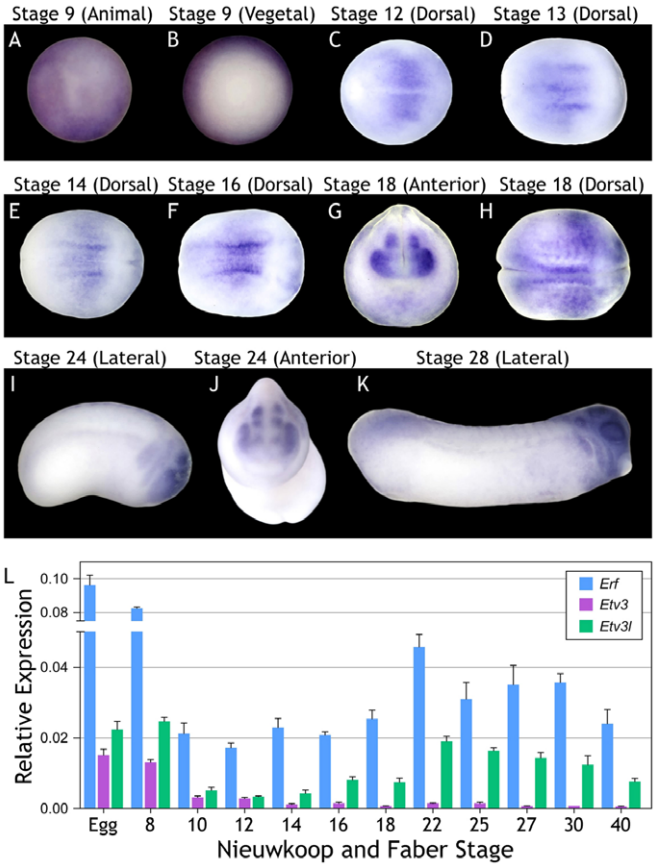

Fig. 3. Expression of *Erf*, *Etv3* and *Etv3l* across developmental time. (**A-K**) Whole-mount *in situ* hybridization of *Erf* mRNA expression at developmental stages 9, 12, 13, 14, 16, 18, 24 and 28. Dorsal and lateral views are shown with anterior towards the right. (**L**) QPCR showing *Erf*, *Etv3* and *Etv3l* gene expression over developmental time. The *y*-axis represents $2^{-\Delta Ct}$ values, adjusted for primer efficiency (Pfaffl, 2001), normalized to the reference gene *Histone H4*.

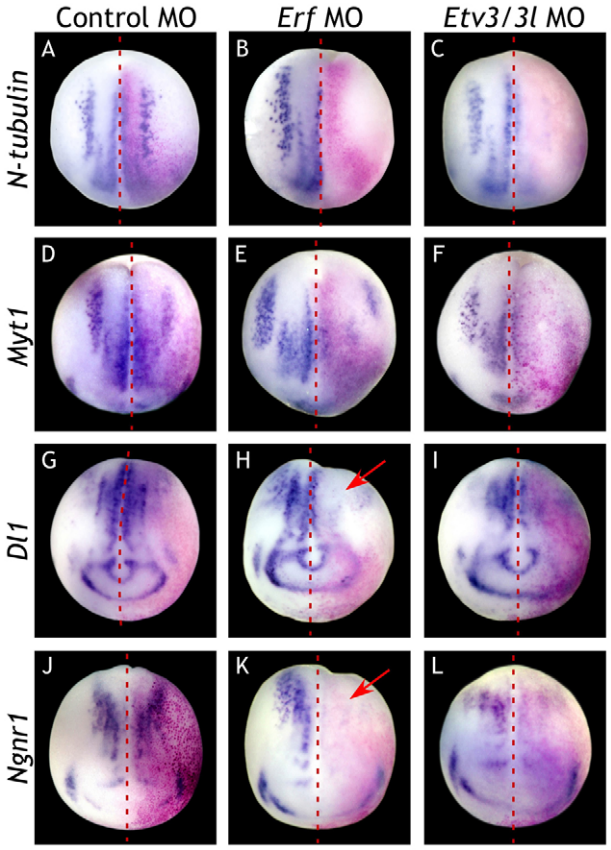

Fig. 4. ERF or ETV3/3L knockdown inhibits the neural differentiation pathway. Embryos were injected unilaterally at the two- or four-cell stage. The injected side is indicated by the magenta lineage tracer. (**A**,**D**,**G**,**J**) Control expression of *N-tubulin*, *Myt1*, *Dl1* and *Ngnr1*. (**B**,**E**,**H**,**K**) Embryos injected with 20 ng *Erf* MO showed reduction of *N-tubulin* (18/19), *Myt1* (11/13), *Dl1* (8/10) and *Ngnr1* (10/11). (**C**,**F**,**I**,**L**) Embryos injected with 20 ng *Etv3/3l* AUG MO showed reduction of *N-tubulin* (23/25), *Myt1* (19/20), *Dl1* (38/44) and *Ngnr1* (20/26). Embryos are shown in dorsal view at stage 14; anterior is at the bottom. Red arrows indicate areas where neural fold elevation is reduced (see supplementary material Fig. S9).

but is absent from the cement gland (Fig. 3G-K). mRNA encoding the DEAD-box protein DDx20, which interacts with and promotes the repressive function of ERF and ETV3 (Klappacher et al., 2002), is expressed in the neural plate (supplementary material Fig. S1E). *Erf*, *Etv3* and *Etv3l* are expressed as maternal transcripts (Fig. 3L). *Erf* mRNA is more abundant than *Etv3l*, which is much more abundant than *Etv3* throughout all stages of development analyzed (Fig. 3L).

ERF or ETV3/3L knockdown inhibit the neural differentiation pathway

As *Erf*-MO and *Etv3/3l*-MO-injected embryos were not responsive to touch, we asked whether loss of function altered primary neurogenesis. Microinjection of *Erf*-MO or *Etv3/3l*-MO resulted in the loss of *N-tubulin* expression (Fig. 4B,C). Two different *Erf*-MOs produced the same phenotype (supplementary material Fig. S7A,B) as did the *Etv3* and *Etv3l* AUG MOs (supplementary material Fig. S7C,D). We combined the *Etv3/3l* MOs in some figures (Figs 4, 5; supplementary material Fig. S6) because we believed at the time that both *Etv3* isoforms might be RA responsive. Extensive experimentation later revealed that only *Etv3l* is RA responsive. However, since the phenotype of both knockdowns is the same (supplementary material Fig. S7C,D), we mixed the MOs for all early experiments, and this is designated *Etv3/3l* MO.

As the loss of *N-tubulin* in *Erf*-MO and *Etv3/3l*-MO phenocopied embryos injected with dominant-negative RARα (Blumberg et al., 1997) or with *Rar* MOs (Fig. 1E,F), or embryos treated with the RAR antagonists Ro 41-5253 (Franco et al., 1999) or AGN193109 (Fig. 1C), we infer that *Erf* and *Etv3/3l* act downstream of RA signaling. In support of this, loss of *Erf* or *Etv3l* rescued the extra/ectopic neurons phenotype generated by VP16-RARα/γ mRNA (Blumberg et al., 1997) (supplementary material Fig. S8) or by TTNPB (Fig. 6). We next tested where in the neurogenic pathway ETS repressors act, compared with when RARs act, by analyzing the effects of ERF and ETV3/3L knockdown on other genes in the neurogenic pathway. The neural differentiation genes *Myt1* (Fig. 4E,F) and *Dl1* (Fig. 4H,I), and the proneural gene *Ngnr1* (Fig. 4K,L) were all knocked down, suggesting that *Erf* and *Etv3/3l* act early in primary neurogenesis.

Microinjection of the *Erf* MO reduced neural fold elevation (Fig. 4H,K, red arrows) compared with controls. We used *Aquaglyceroporin 3* (*Aqp3*), which marks the tips of the neural folds (Cornish et al., 2009) and *Neogenin*, which is required for neural fold elevation (Kee et al., 2008), to demonstrate this neural tube

defect in *Erf* MO embryos at stage 14 (supplementary material Fig. S9). This neural tube defect was resolved by stage 22 (supplementary material Fig. S9E), and embryos appeared morphologically normal at the tadpole stage but were unresponsive to touch. Hence, we conclude that *Erf* knockdown does not simply delay neurogenesis on the injected side. In support of this, stage 22 embryos have diminished N-tubulin expression on the injected side (supplementary material Fig. S10).

ERF or ETV3/3L knockdown expands expression of neural progenitor markers

Erf and *Etv3* are cell cycle inhibitors in certain cell types (Klappacher et al., 2002; Sawka-Verhelle et al., 2004; Sgouras et al., 1995; Verykokakis et al., 2007). Since RARs act early in the neuronal differentiation pathway, we hypothesized that ERF and ETV3/3L might act downstream of RARs to promote cell cycle exit and increase neuronal differentiation. Knockdown of *Erf* or *Etv3/3l* should affect early acting genes that increase the proliferation of neural precursors while inhibiting neuronal differentiation.

Neural induction leads to the upregulation of *Zic1*, *Zic3* and *Foxd4l1*, which allows ectodermal cells to commit to the neural fate and promotes expression of genes that maintain proliferation in the neural plate at the expense of differentiation (reviewed in Aruga and Mikoshiba, 2011; Moody and Je, 2002; Rogers et al., 2009). *Erf*-MO and *Etv3/3l*-MO embryos exhibited lateral expansion of *Zic1* (Fig. 5B,C) and *Zic3* (Fig. 5E,F) but posterior reduction of *Zic1* (Fig. 5B,C). The characteristic dorsal striped expression pattern of *Zic3* (Fig. 5D) was lost (Fig. 5E,F). *Erf* and *Etv3* knockdown expanded *Foxd4l1* (Fig. 5H,I), indicating that *Erf* and *Etv3* function early in the pathway to inhibit genes responsible for early neural stabilization and proliferation.

Foxd4l1 upregulates *Geminin* and *Zic2*, genes that are known to maintain the neuroectoderm in an immature proliferative state (reviewed by Moody and Je, 2002; Rogers et al., 2009). *Erf* and *Etv3/3l* MOs expanded *Geminin* and *Zic2* expression domains (Fig. 5K,L,N,O). These embryos also exhibited blurring of the dorsal striped pattern of *Zic2*, similar to the effects on *Zic3* (Fig. 5E,F) and in embryos treated with an RAR antagonist (Franco et al., 1999).

Knockdown of ERF or ETV3L promotes proliferation in the neural plate

SoxB1 family genes (e.g. *Sox2*, *Sox3*) are downstream of *Foxd4l1*, *Geminin* and *Zic2* (reviewed by Moody and Je, 2002; Rogers et al., 2009), maintain neural progenitor cells in a proliferative state, and are downregulated during neural differentiation (Archer et al., 2011; Bylund et al., 2003; Miyagi et al., 2009; Wegner and Stolt, 2005). Injection of *Rarα*-MO, *Rarγ*-MO, *Erf*-MO or *Etv3/3l*-MO led to expanded *Sox3* expression (supplementary material Fig. S6D-I). We interpreted the expanded neural plate (as indicated by *Sox3*) and the broadened expression of *Geminin*, *Zic2* and *Foxd4l1* to indicate that the neural plate in these MO-injected embryos remains in an immature proliferative state.

To test this inference, we performed whole-mount immunohistochemisty on injected embryos, detecting proliferating cells with an antibody against phosphorylated *Histone H3* (at Ser10) (Hendzel et al., 1997) or an antibody against PCNA (Mathews et al., 1984). Figure 7 shows representative images of embryos taken in bright-field (Fig. 7A,D,G) and fluorescence (Fig. 7B,E,H). Knockdown of *Erf* or *Etv3l* produced significantly more phospho-*Histone H3*+ staining in the neural plate compared with control-MO (Fig. 7C,F,I). This effect is specific to the neural plate as there was no effect on lateral, non-neural expression of phospho-*Histone H3* (supplementary material Fig. S11). Knockdown of *Erf* or *Etv3l* produced significantly more PCNA staining in the neural plate compared with control-MO (supplementary material Fig. S12).

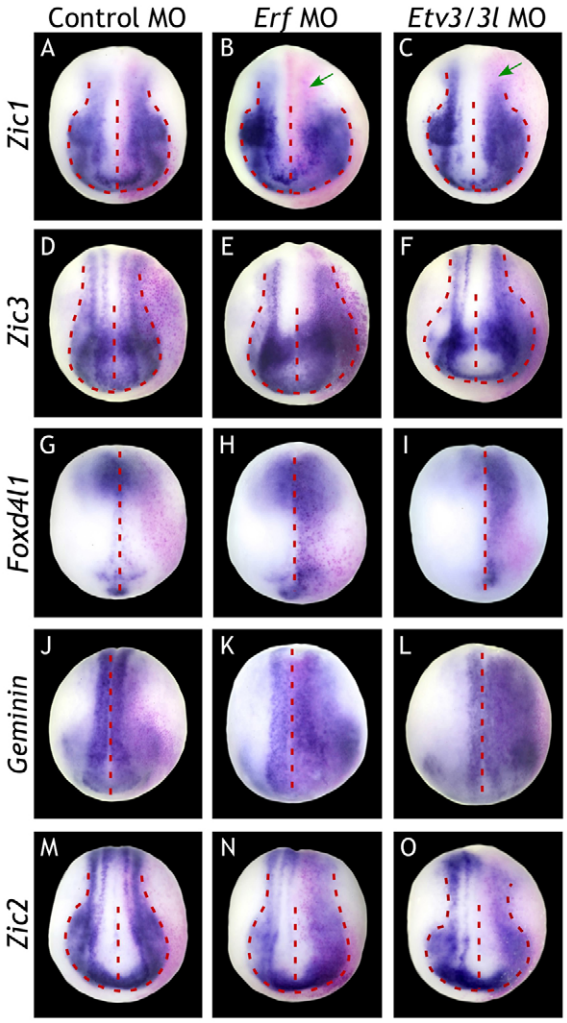

Fig. 5. ERF or ETV3/3L knockdown expands expression of *Zic1*, *Zic2*, *Zic3*, *Geminin* and *Foxd4l1* in the anterior/dorsal region. Embryos were injected unilaterally at the two- or four-cell stage. The injected side is indicated by the magenta lineage tracer. (**A**,**D**,**G**,**J**,**M**) Control expression of *Zic1*, *Zic2*, *Zic3*, *Geminin* and *Foxd4l1*. (**B**,**E**,**H**,**K**,**N**) Embryos injected with 10 ng *Erf* MO showed lateral expansion (13/14) and posterior reduction (13/14, green arrow) of *Zic1*; stripe blurring (23/23) and posterior reduction (10/23) of *Zic2*; stripe blurring (14/21) and posterior reduction (6/21) of *Zic3*; and expansion of *Foxd4l1* (10/16) and *Geminin* (16/22). (**C**,**F**,**I**,**L**,**O**) Embryos injected with 20 ng *Etv3/3l* MO showed lateral expansion (12/15) and posterior reduction (12/15, green arrow) of *Zic1*; stripe blurring (14/14), lateral expansion (5/14) and posterior reduction (10/14) of *Zic2*; stripe blurring (14/14), lateral expansion (18/21) and posterior reduction (8/21) of *Zic3*; and expansion of *Foxd4l1* (16/20) and *Geminin* (16/16). Embryos are shown in dorsal view at stage 14; anterior is at the bottom.

Erf overexpression leads to an increase of neurons

Erf loss of function phenocopied RAR loss of function (increased proliferation and inhibited neuronal differentiation); thus, overexpression of *Erf* mRNA should produce more primary neurons in the neural plate. However, unilateral overexpression of *Erf*

mRNA inhibited expression of *N-tubulin* (not shown). FGF signaling plays at least two roles in neurogenesis: (1) FGF promotes neural induction and posteriorizes the neuroectoderm; and (2) FGF promotes proliferation of neural progenitors, delaying neuronal differentiation. We hypothesized that overexpression of *Erf* interfered with the first function, inhibiting *Ets* genes downstream of FGF signaling required for neural induction (Bertrand et al., 2003). This would lead to a paucity of neurogenic precursors and thus fewer primary neurons.

We used hormone-inducible constructs to allow precise temporal control of ERF activity, in order to distinguish the effects of *Erf* on neural induction from effects on neuronal differentiation. Fusion of ERF to the ligand-binding domain of the human glucocorticoid receptor (hGR) sequesters ERF in the cytoplasm in the absence of dexamethasone (DEX) (Kolm and Sive, 1995). DEX treatment releases ERF, allowing it to enter the nucleus. ERF is exported from the nucleus upon phosphorylation by ERK (extracellular signal-regulated kinase), therefore we designed mutated constructs that manipulate ERK phosphorylation. ERF is phosphorylated at Thr^{526}, Ser^{161}, Ser^{246} and Ser^{251} in rodent fibroblasts; alanine substitutions at any of these positions decreased nuclear export and increased ERF-mediated repression (Le Gallic et al., 1999). Only Ser^{246} and Ser^{251} and the surrounding residues required for phosphorylation by ERK are conserved in *Xenopus*, chick and zebrafish. We designed a 'constitutively nuclear' construct to mimic permanently the unphosphorylated state ($Ser^{246,251} \rightarrow Ala^{246,251}$), such that ERF is maintained in the nucleus and increases repression. A phosphomimetic ($Ser^{246,251} \rightarrow Glu^{246,251}$) mutant that is constitutively exported from the nucleus (inhibiting repression) was also produced (Wagner et al., 2004). These *Erf* constructs demonstrated the appropriate subcellular localization in the presence and absence of DEX (supplementary material Fig. S13).

mRNAs encoding hGR-ERF fusion proteins were unilaterally microinjected into two- or four-cell embryos, treated with dexamethasone after the beginning of neural induction (stage 11) and fixed at stage 14. Whole-mount *in situ* hybridization with *N-tubulin* revealed that overexpression of *hGR-Erf* ($Ser^{246,251} \rightarrow Ala^{246,251}$) after neural induction led to more primary neurons (supplementary material Fig. S14A; Fig. S15B,D). The *hGR-Erf* ($Ser^{246,251} \rightarrow Glu^{246,251}$) mutant did not affect the number of neurons, presumably because it is transported out of the nucleus and is unable to act as a transcriptional repressor (supplementary material Fig. S14B; Fig. S15F,H). DMSO treatment did not alter the number of neurons (supplementary material Fig. S14; Fig. S15A,C,E,G). To demonstrate that *Erf* acts downstream of RAR, we attempted to rescue the loss of *N-tubulin* in RARγ-MO embryos with hGR-*Erf* ($Ser^{246,251} \rightarrow Ala^{246,251}$) mRNA. We observed a partial rescue of *N-tubulin* in dexamethasone-treated embryos (supplementary material Fig. S16).

We examined *N-tubulin* expression at a slightly earlier stage (stage 13/13.5) to determine whether overexpression of hGR-*Erf* ($Ser^{246,251} \rightarrow Ala^{246,251}$) caused precocious neurogenesis. When embryos injected with hGR-*Erf* (S→A) were treated with dexamethasone at stage 10.5 or stage 11, we noticed precocious neurogenesis on the injected side in 27-28% of the embryos (Fig. 8E,F,H,I). Overexpression of *hGR-Erf* (S→A) decreased proliferation on the injected side of dexamethasone-treated embryos (supplementary material Fig. S17D-F). When embryos were treated at stage 9 with dexamethasone, knock down of *N-tubulin* was observed, as expected, presumably because *Erf* interfered with the early action of FGF on neural induction (Fig. 8B,C). When embryos were treated with dexamethasone after stage 11, no precocious neurogenesis was observed. We infer that *Erf* was released to function in the nucleus too late to affect neuronal differentiation (Fig. 8K,L). DMSO vehicle treatment did not alter the number of neurons (Fig. 8A,C,D,F,G,I,J,L) or proliferation (supplementary material Fig. S17A-C).

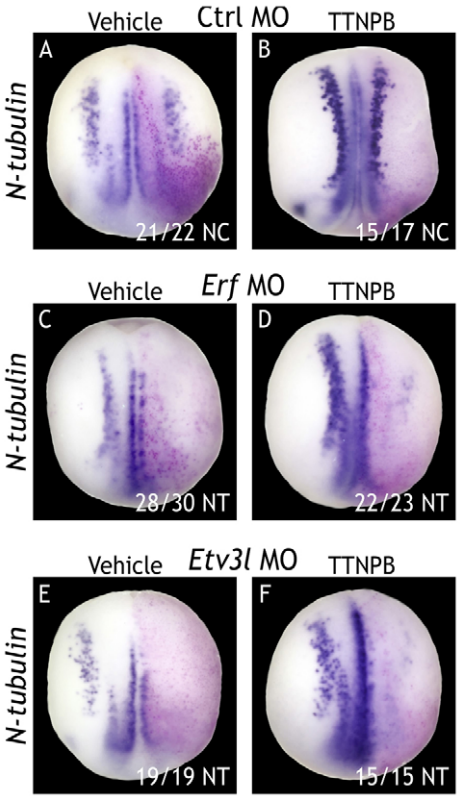

Fig. 6. ERF or ETV3L knockdown rescues the extra/ectopic neuron phenotype generated by TTNPB. All embryos were injected unilaterally at the two- or four-cell stage. The injected side is indicated by the magenta *β-gal* mRNA lineage tracer. Embryos were treated at stage 7/8 with TTNPB or control vehicle (0.1% ethanol). (**A**,**B**) 10 ng control MO does not change expression of *N-tubulin* (NC, no change). (**C**,**D**) 10 ng *Erf* MO rescues (96%) the TTNPB extra/ectopic neuron phenotype (NT, no tubulin). (**E**,**F**) 20 ng *Etv3l* MO completely rescues (100%) the TTNPB phenotype. Embryos are shown in dorsal view with anterior at the bottom, at stage 14.

DISCUSSION

RAR signaling promotes neuronal differentiation

Developing systems maintain a dynamic balance between cell proliferation and differentiation, yet the molecular mechanisms regulating this equilibrium are poorly understood. Mutually inhibitory interactions between factors promoting proliferation (e.g. FGFs) versus differentiation (e.g. RA), and cell cycle genes involved have been described in a few systems, including neuronal progenitor cells (Chen et al., 2012; Diez del Corral et al., 2003; Seo et al., 2005a). Little is known about the molecular nature of the switch that controls the shift between proliferation of neural precursors and their entry into the neuronal differentiation pathway (Kaldis and Richardson, 2012).

RAR signaling plays a significant role in patterning the neural plate and promoting primary neurogenesis. Knockdown of RARα or RARγ independently led to loss of primary neurons, supporting our previous observation that *Xenopus* RAR subtypes exhibit

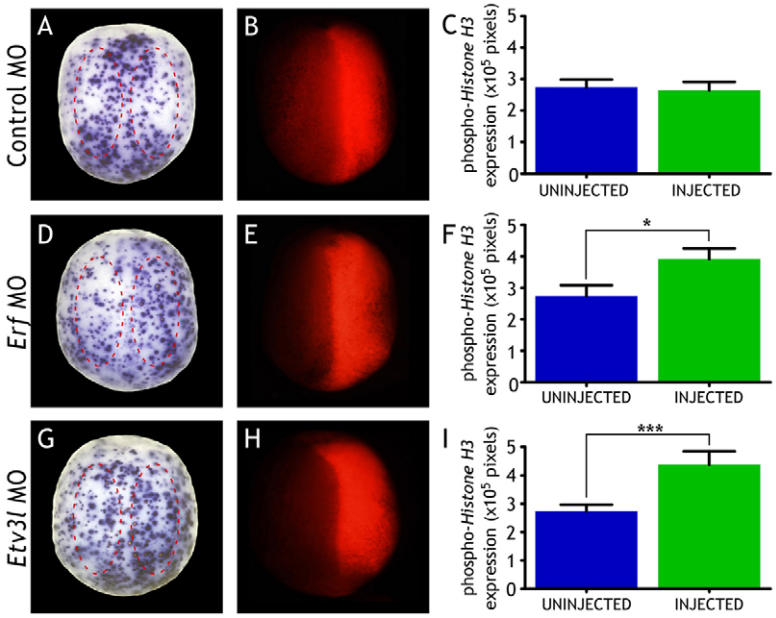

Fig. 7. ERF or ETV3L knockdown increases proliferation in the neural plate. Embryos were injected unilaterally at the 2- or 4-cell stage. The injected side is indicated by the red fluorescent lineage tracer. Representative photographs in bright-field (A,D,G) and fluorescence (B,E,H) are shown. Quantitation of phospho-*Histone H3* nuclei staining (scored blindly within dotted line ovals and normalized to account for differences in staining intensity) for all embryos in the experiment is provided in bar graphs (C,F,I). Embryos are shown in dorsal view at stage 14; anterior is at the bottom. (**A-C**) Embryos injected with 10 ng control MO showed no significant difference in the number of phospho-*Histone H3* nuclei on the injected versus the uninjected side (n=27; P=0.71). (**D-F**) Embryos injected with 10 ng *Erf* MO showed an increased number of phospho-*Histone H3* nuclei on the injected side (n=23; *P=0.022). (**G-I**) Embryos injected with 10 ng *Etv3l* MO showed an increased number of phospho-*Histone H3* nuclei on the injected side (n=26; ***P=0.0009).

temporal and spatial regulation of different target genes (Koide et al., 2001; Shiotsugu et al., 2004). As RA cannot neuralize naïve ectoderm (Blumberg et al., 1997; Sharpe and Goldstone, 1997), we predicted that the decreased number of primary neurons due to RAR loss of function resulted from a failure of neuronal differentiation rather than a loss of neural competence. We found that loss of the differentiation signal from RAR caused expansion of markers of neural progenitors and neural stabilization (*Geminin*, *Foxd4l1* and *Sox3*). Increasing RA signaling reduced *Geminin* and *Foxd4l1* expression while increasing neuronal differentiation. Hence, we inferred that *Rarα* and *Rarγ* play early roles in neural differentiation by inhibiting proliferation of neural progenitors.

Erf and Etv3 are RA responsive and promote neuronal differentiation

Our results showed that ETS repressors are effectors of RA signaling that promote primary neurogenesis. Treatment of embryos with TTNPB or AGN193109 significantly altered the *Erf* expression domain, and *Rarα* or *Rarγ* were required for *Erf* expression. Knockdown of ERF or ETV3/3L caused embryos to be unresponsive to touch and primary neurons were lost, phenocopying RAR loss of function. By contrast, temporally controlled *Erf* gain of function increased the number of neurons at stage 14, and led to precocious neurogenesis at slightly earlier stages. We showed that Ets repressors are downstream of RAR in neuronal differentiation. Loss of either ERF or ETV3L blocked the production of excess neurons generated by a constitutively active VP16-RAR or by TTNPB treatment. We predict that the connection between RAR signaling and Ets-repressors will prove to be important in other biological processes in the future.

ERF or ETV3/3L knockdown expand expression of neural progenitor markers

As RAR loss of function caused expansion of *Geminin*, *Foxd4l1* and *Sox3*, we hypothesized that *Erf* and *Etv3/3l* also act early in the neurogenic pathway. After neural tissue is induced via BMP inhibition and active FGF signaling, *Zic1*, *Zic3* and *Foxd4l1* are upregulated (Marchal et al., 2009; Tropepe et al., 2006; Wills et al., 2010). *Foxd4l1* and *Zic3* are downstream targets of FGF signaling (Branney et al., 2009; Lee et al., 2009; Marchal et al., 2009; Yan et al., 2010), whereas *Zic1* is an immediate early gene of BMP inhibition and is driven by a BMP inhibitor-responsive promoter module (Tropepe et al., 2006). *Zic1* and *Zic3* stabilize the neural fate immediately after neural induction, promoting plasticity of neural progenitors and inhibiting differentiation (Aruga, 2004; Aruga and Mikoshiba, 2011; Aruga et al., 2002; Merzdorf, 2007). *Zic1* is highly expressed in human ESC-derived neural rosettes and in proliferating neural stem cell progenitors (Elkabetz et al., 2008; Tabar et al., 2005). *Zic3* is a direct target of pluripotency factors in stem cells, and is diminished after differentiation with RA (Lim et al., 2007). Knockdown of ERF or ETV3/3L caused marked expansion of *Foxd4l1*, *Zic1* and *Zic3*; hence, *Erf* and *Etv3/3l* regulate important factors that mediate the early transcriptional response downstream of BMP inhibition and FGF signaling in neural induction.

Knockdown of ERF or ETV3/3L expanded the *Geminin* and *Zic2* expression domain comparable with that observed in *Rarα*-MO and *Rarγ*-MO embryos. Expansion of *Zic2* leads to the inhibition of *Xngnr-1*, which normally induces expression of *Myt-1* and *Delta-1* to promote neurogenesis (Bellefroid et al., 1996; Brewster et al., 1998; Chitnis et al., 1995). *Geminin* plays a primary role in maintaining neuroectoderm in an 'immature state', conferring a reduced response to differentiation signals (Neilson et al., 2012; Yan et al., 2009; Yan et al., 2010). *Geminin* is highly expressed in proliferating neural progenitors (Spella et al., 2007), where it interacts with *Brahma-related gene 1* to inhibit neuronal differentiation and increase proliferation (Seo et al., 2005a; Seo et al., 2005b). *Geminin* regulates the expression of *Sox3* in a positive-feedback loop and is thought to postpone lineage commitment by stabilizing repressive chromatin marks to promote cellular plasticity (Lim et al., 2011). We infer that *Erf* and *Etv3/3l* restrict *Zic2* and *Geminin* expression in the neural plate, inhibiting neural progenitor plasticity and proliferation, and defining cell fate and promoting lineage commitment.

Erf and Etv3l inhibit proliferation in the neural plate

RA is known to regulate the expression of genes that facilitate cell cycle exit and differentiation (Andrews, 1984; Rhinn and Dollé, 2012). FGF signaling promotes neural progenitor survival and proliferation in early neural tissue and in the mammalian brain

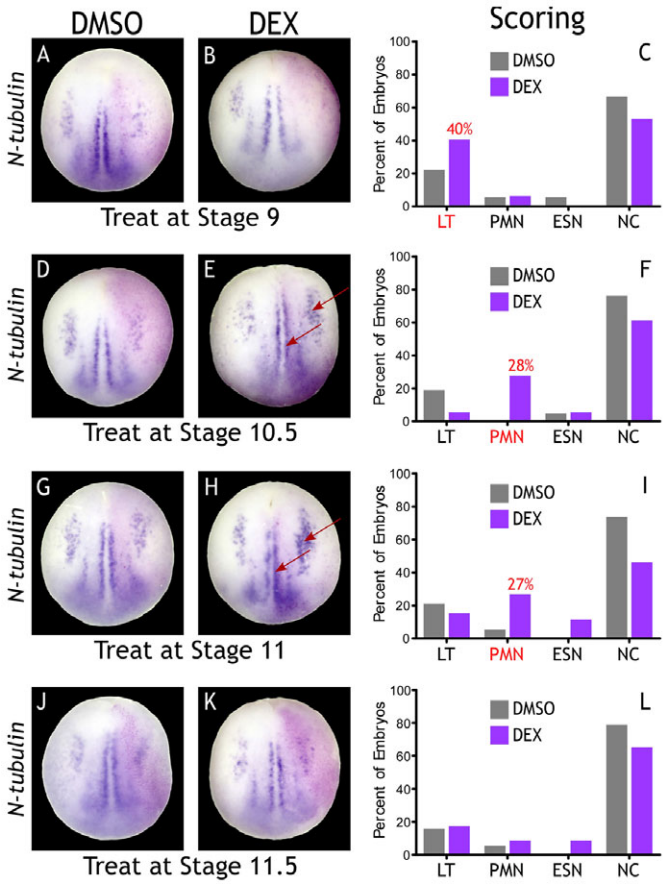

Fig. 8. ERF gain of function leads to precocious neurogenesis under appropriate conditions. (A-L) All embryos were injected unilaterally with 0.1 ng *hGR-Erf* ($S^{246,251}$ $A^{246,251}$) mRNA at the two- or four-cell stage, then treated with 10 µM dexamethasone (DEX) or 0.1% DMSO vehicle at various stages. The injected side is indicated by the magenta *β-gal* mRNA lineage tracer. (**A**,**D**,**G**,**J**) DMSO-treated embryos. (**B**) Dexamethasone treatment at stage 9 produced reduction of *N-tubulin* in 40% of embryos. (**E**) Dexamethasone treatment at stage 10.5 produced precocious neurogenesis in 28% of embryos. (**H**) Dexamethasone treatment at stage 11 produced precocious neurogenesis in 27% of embryos. (**K**) Embryos treated with dexamethasone at stage 11.5 were mostly unchanged. The red arrows indicate the increase in *N-tubulin* expression. (**C**,**F**,**I**,**L**) Scoring of embryos in A-K: LT, low tubulin; PMN, premature neurogenesis; ESN, extra sensory neurons; NC, no change. All embryos are shown in dorsal view with anterior at the bottom, at stage 13/13.5.

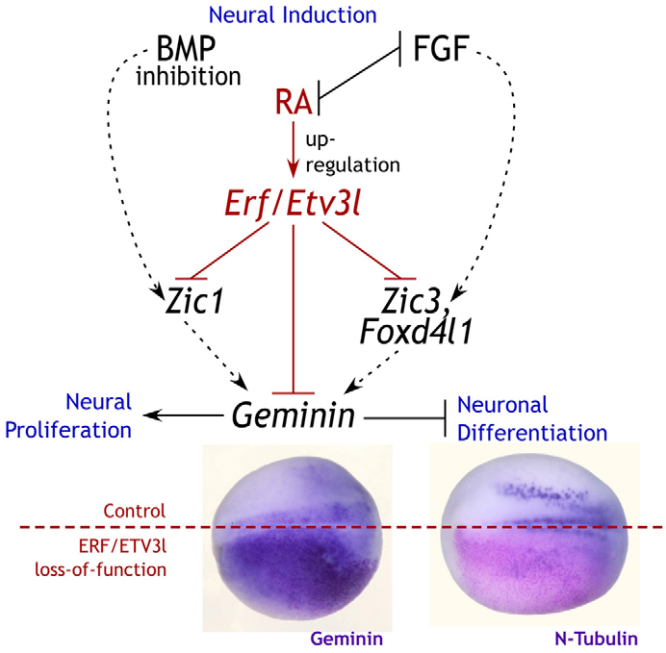

Fig. 9. RA and ERF/ETV3L action in primary neurogenesis. The mutual inhibitory interactions between FGF and RAR signaling have been discussed in this paper and elsewhere (Diez del Corral and Storey, 2004; Moreno and Kintner, 2004). FGF signaling and BMP inhibition (required for neural induction) leads to the upregulation of neural progenitor and pro-proliferation genes such as *Zic1*, *Zic3*, *Foxd4l1* and *Geminin*. RA upregulates ETS repressors *Erf* and *Etv3l*, which function to inhibit these genes and to promote neuronal differentiation. Loss of either ERF or ETV3L leads to expansion of *Geminin* and loss of *N-Tubulin* on the injected side of the embryo. Embryos are shown in dorsal view at stage 14; anterior is on the right.

(Chen et al., 2012; Marchal et al., 2009; Mason, 2007), and uses ETS transcription factors as terminal effectors (Bertrand et al., 2003; Sharrocks, 2001; Wasylyk et al., 1998). ERF and ETV3 recognize *Ets1/2* consensus sites, which are downstream of FGF signaling *in vivo*, that are often found in the regulatory regions of positive cell cycle genes such as *c-Myc*, *c-Myb*, *p54* and *Cdc-2* (Carlson et al., 2011; Hester et al., 2007; Klappacher et al., 2002).

We propose that *Erf* and *Etv3/3l* play a similar role in the neuroectoderm, inhibiting proliferation of neural progenitors by restricting expression of genes (e.g. *Foxd4l1*, *Geminin*, *Sox3*, *Zic1* and *Zic3*) that stabilize the neural fate and prevent differentiation by maintaining plasticity and/or proliferation of neural progenitors. ERF or ETV3L knockdown elicited a significant increase in cell proliferation in the neural plate, whereas overexpression of ERF produced the opposite result. We conclude that ERF and ETV3/3L play key roles in terminating the cell cycle to facilitate neuronal differentiation.

Erf and *Etv3l* as potential mediators of RA and FGF crosstalk

FGF signaling and BMP inhibition initiate neural induction, leading to the upregulation of genes (such as *Foxd4l1*, *Zic1*, *Zic2*, *Zic3*, *Geminin* and *Sox3*) that promote and maintain neural competence. This early gene network generates a neural progenitor identity within the neuroectoderm characterized by a stem-like fate of plasticity and proliferation. When the neuroectoderm is fully stabilized, it is equally important for this gene network to be downregulated for differentiation to occur. Retinoic acid receptors and their effectors, *Erf* and *Etv3l*, are expressed at the correct time and place to interfere with the action of neural progenitor genes and facilitate neuronal differentiation. Loss of ERF or ETV3L prolongs neural progenitor identity, increasing proliferation and preventing the development of mature neurons. ERF overexpression causes the opposite effect, increasing the number of primary neurons.

We infer that ETS repressors, *Erf* and *Etv3l*, sit at the intersection of proliferation and differentiation. Fig. 9 summarizes our model for how RA and *Erf/Etv3l* regulate the proliferation/differentiation switch in primary neurogenesis. RAR action promotes the expression of *Erf* and *Etv3l* to inhibit the cell cycle downstream of FGF in the neuroectoderm. Whether *Foxd4l1*, *Zic1*, *Zic2*, *Zic3*, *Geminin* and *Sox3* are regulated directly by ETS repressors at the transcriptional level remains an unanswered question. Although it is well known that

FGF signaling employs ETS proteins in signal transduction, BMP signaling also uses ETS factors that act in synergy with Smad proteins (Koinuma et al., 2009; Morikawa et al., 2011). The BMP inhibitory response module that drives *Zic1* expression contains multiple, functional ETS-binding sites (Tropepe et al., 2006). *Erf* and *Etv3/3l* could play a direct role, binding ETS sites in the regulatory regions of neural progenitor genes (such as *Foxd4l1*, *Zic2* and *Geminin*). Alternatively, *Erf* and *Etv3/3l* could simply promote cell cycle exit, terminating expression of genes associated with neural progenitor identity and facilitating differentiation. The results presented above demonstrate that RAR negatively influences FGF signaling by upregulating *Erf* and *Etv3l* to repress genes that stimulate neural progenitor fate, establishing an important new role for opposing RA and FGF signals in primary neurogenesis.

Acknowledgements
We thank Dr Tom Schilling (UCI, Irvine, CA, USA) for the use of his fluorescence microscope, and Dr Pierre Le Pabic and Kelly Radtke in his lab for help with photography and Velocity software. We thank Dr Ken Cho (UCI) for the use of his GFP microscope and Dr Ira Blitz in his lab for help with photography. We thank former UCI undergraduate student Jennifer Dean for technical help during the early stages of this study.

Funding
Supported by grants from the National Science Foundation (NSF) [IOS-0719576, IOS-1147236] to B.B. A.J. was a pre-doctoral trainee of the NSF IGERT program [DGE 0549479].

Competing interests statement
The authors declare no competing financial interests.

Author contributions
M.T. performed initial Etv3/3l staging and Etv3l MO WISH. C.C., R.A.,and S.L. conducted WISH, QPCR, immunohistochemistry, cloning and photography with Etv3/3l MO, Erf MO and hGR-Erf. A.J. and B.B. contributed to and supervised all experiments, wrote, edited and submitted the manuscript.

Supplementary material
Supplementary material available online at
http://dev.biologists.org/lookup/suppl/doi:10.1242/dev.093716/-/DC1

References

Anderson, R. B. and Holt, C. E. (2002). Expression of UNC-5 in the developing Xenopus visual system. *Mech. Dev.* **118**, 157-160.
Andrews, P. W. (1984). Retinoic acid induces neuronal differentiation of a cloned human embryonal carcinoma cell line in vitro. *Dev. Biol.* **103**, 285-293.
Archer, T. C., Jin, J. and Casey, E. S. (2011). Interaction of Sox1, Sox2, Sox3 and Oct4 during primary neurogenesis. *Dev. Biol.* **350**, 429-440.
Arima, K., Shiotsugu, J., Niu, R., Khandpur, R., Martinez, M., Shin, Y., Koide, T., Cho, K. W., Kitayama, A., Ueno, N. et al. (2005). Global analysis of RAR-responsive genes in the Xenopus neurula using cDNA microarrays. *Dev. Dyn.* **232**, 414-431.
Aruga, J. (2004). The role of Zic genes in neural development. *Mol. Cell. Neurosci.* **26**, 205-221.
Aruga, J. and Mikoshiba, K. (2011). Role of BMP, FGF, calcium signaling, and Zic proteins in vertebrate neuroectodermal differentiation. *Neurochem. Res.* **36**, 1286-1292.
Aruga, J., Tohmonda, T., Homma, S. and Mikoshiba, K. (2002). Zic1 promotes the expansion of dorsal neural progenitors in spinal cord by inhibiting neuronal differentiation. *Dev. Biol.* **244**, 329-341.
Balmer, J. E. and Blomhoff, R. (2002). Gene expression regulation by retinoic acid. *J. Lipid Res.* **43**, 1773-1808.
Bellefroid, E. J., Bourguignon, C., Hollemann, T., Ma, Q., Anderson, D. J., Kintner, C. and Pieler, T. (1996). X-MyT1, a Xenopus C2HC-type zinc finger protein with a regulatory function in neuronal differentiation. *Cell* **87**, 1191-1202.
Bertrand, V., Hudson, C., Caillol, D., Popovici, C. and Lemaire, P. (2003). Neural tissue in ascidian embryos is induced by FGF9/16/20, acting via a combination of maternal GATA and Ets transcription factors. *Cell* **115**, 615-627.
Blumberg, B., Bolado, J., Jr, Moreno, T. A., Kintner, C., Evans, R. M. and Papalopulu, N. (1997). An essential role for retinoid signaling in anteroposterior neural patterning. *Development* **124**, 373-379.
Branney, P. A., Faas, L., Steane, S. E., Pownall, M. E. and Isaacs, H. V. (2009). Characterisation of the fibroblast growth factor dependent transcriptome in early development. *PLoS ONE* **4**, e4951.
Brewster, R., Lee, J. and Ruiz i Altaba, A. (1998). Gli/Zic factors pattern the neural plate by defining domains of cell differentiation. *Nature* **393**, 579-583.
Bylund, M., Andersson, E., Novitch, B. G. and Muhr, J. (2003). Vertebrate neurogenesis is counteracted by Sox1-3 activity. *Nat. Neurosci.* **6**, 1162-1168.
Carlson, S. M., Chouinard, C. R., Labadorf, A., Lam, C. J., Schmelzle, K., Fraenkel, E. and White, F. M. (2011). Large-scale discovery of ERK2 substrates identifies ERK-mediated transcriptional regulation by ETV3. *Sci. Signal.* **4**, rs11.
Chalmers, A. D., Welchman, D. and Papalopulu, N. (2002). Intrinsic differences between the superficial and deep layers of the Xenopus ectoderm control primary neuronal differentiation. *Dev. Cell* **2**, 171-182.
Chamorro-Garcia, R., Kirchner, S., Li, X., Janesick, A., Casey, S. C., Chow, C. and Blumberg, B. (2012). Bisphenol A diglycidyl ether induces adipogenic differentiation of multipotent stromal stem cells through a peroxisome proliferator-activated receptor gamma-independent mechanism. *Environ. Health Perspect.* **120**, 984-989.
Chen, J., Lai, F. and Niswander, L. (2012). The ubiquitin ligase mLin41 temporally promotes neural progenitor cell maintenance through FGF signaling. *Genes Dev.* **26**, 803-815.
Chitnis, A., Henrique, D., Lewis, J., Ish-Horowicz, D. and Kintner, C. (1995). Primary neurogenesis in Xenopus embryos regulated by a homologue of the Drosophila neurogenic gene Delta. *Nature* **375**, 761-766.
Cornish, E. J., Hassan, S. M., Martin, J. D., Li, S. and Merzdorf, C. S. (2009). A microarray screen for direct targets of Zic1 identifies an aquaporin gene, aqp-3b, expressed in the neural folds. *Dev. Dyn.* **238**, 1179-1194.
Denny, P., Swift, S., Brand, N., Dabhade, N., Barton, P. and Ashworth, A. (1992). A conserved family of genes related to the testis determining gene, SRY. *Nucleic Acids Res.* **20**, 2887.
Diez del Corral, R. and Storey, K. G. (2004). Opposing FGF and retinoid pathways: a signalling switch that controls differentiation and patterning onset in the extending vertebrate body axis. *Bioessays* **26**, 857-869.
Diez del Corral, R., Olivera-Martinez, I., Goriely, A., Gale, E., Maden, M. and Storey, K. (2003). Opposing FGF and retinoid pathways control ventral neural pattern, neuronal differentiation, and segmentation during body axis extension. *Neuron* **40**, 65-79.
Dorey, K. and Amaya, E. (2010). FGF signalling: diverse roles during early vertebrate embryogenesis. *Development* **137**, 3731-3742.
Duester, G. (2008). Retinoic acid synthesis and signaling during early organogenesis. *Cell* **134**, 921-931.
Elkabetz, Y., Panagiotakos, G., Al Shamy, G., Socci, N. D., Tabar, V. and Studer, L. (2008). Human ES cell-derived neural rosettes reveal a functionally distinct early neural stem cell stage. *Genes Dev.* **22**, 152-165.
Franco, P. G., Paganelli, A. R., López, S. L. and Carrasco, A. E. (1999). Functional association of retinoic acid and hedgehog signaling in Xenopus primary neurogenesis. *Development* **126**, 4257-4265.
Gudas, L. J. (1992). Retinoids, retinoid-responsive genes, cell differentiation, and cancer. *Cell Growth Differ.* **3**, 655-662.
Hellsten, U., Harland, R. M., Gilchrist, M. J., Hendrix, D., Jurka, J., Kapitonov, V., Ovcharenko, I., Putnam, N. H., Shu, S., Taher, L. et al. (2010). The genome of the Western clawed frog Xenopus tropicalis. *Science* **328**, 633-636.
Hendzel, M. J., Wei, Y., Mancini, M. A., Van Hooser, A., Ranalli, T., Brinkley, B. R., Bazett-Jones, D. P. and Allis, C. D. (1997). Mitosis-specific phosphorylation of histone H3 initiates primarily within pericentromeric heterochromatin during G2 and spreads in an ordered fashion coincident with mitotic chromosome condensation. *Chromosoma* **106**, 348-360.
Hester, K. D., Verhelle, D., Escoubet-Lozach, L., Luna, R., Rose, D. W. and Glass, C. K. (2007). Differential repression of c-myc and cdc2 gene expression by ERF and PE-1/METS. *Cell Cycle* **6**, 1594-1604.
Hollenhorst, P. C., McIntosh, L. P. and Graves, B. J. (2011). Genomic and biochemical insights into the specificity of ETS transcription factors. *Annu. Rev. Biochem.* **80**, 437-471.
Janesick, A., Shiotsugu, J., Taketani, M. and Blumberg, B. (2012). RIPPLY3 is a retinoic acid-inducible repressor required for setting the borders of the pre-placodal ectoderm. *Development* **139**, 1213-1224.
Kaldis, P. and Richardson, H. E. (2012). When cell cycle meets development. *Development* **139**, 225-230.
Kee, N., Wilson, N., De Vries, M., Bradford, D., Key, B. and Cooper, H. M. (2008). Neogenin and RGMa control neural tube closure and neuroepithelial morphology by regulating cell polarity. *J. Neurosci.* **28**, 12643-12653.
Klappacher, G. W., Lunyak, V. V., Sykes, D. B., Sawka-Verhelle, D., Sage, J., Brard, G., Ngo, S. D., Gangadharan, D., Jacks, T., Kamps, M. P. et al. (2002). An induced Ets repressor complex regulates growth arrest during terminal macrophage differentiation. *Cell* **109**, 169-180.
Klein, S. L., Strausberg, R. L., Wagner, L., Pontius, J., Clifton, S. W. and Richardson, P. (2002). Genetic and genomic tools for Xenopus research: The NIH Xenopus initiative. *Dev. Dyn.* **225**, 384-391.

Koide, T., Downes, M., Chandraratna, R. A., Blumberg, B. and Umesono, K. (2001). Active repression of RAR signaling is required for head formation. *Genes Dev.* **15**, 2111-2121.
Koinuma, D., Tsutsumi, S., Kamimura, N., Taniguchi, H., Miyazawa, K., Sunamura, M., Imamura, T., Miyazono, K. and Aburatani, H. (2009). Chromatin immunoprecipitation on microarray analysis of Smad2/3 binding sites reveals roles of ETS1 and TFAP2A in transforming growth factor beta signaling. *Mol. Cell. Biol.* **29**, 172-186.
Kolm, P. J. and Sive, H. L. (1995). Efficient hormone-inducible protein function in Xenopus laevis. *Dev. Biol.* **171**, 267-272.
Kroll, K. L., Salic, A. N., Evans, L. M. and Kirschner, M. W. (1998). Geminin, a neuralizing molecule that demarcates the future neural plate at the onset of gastrulation. *Development* **125**, 3247-3258.
Kuo, J. S., Patel, M., Gamse, J., Merzdorf, C., Liu, X., Apekin, V. and Sive, H. (1998). Opl: a zinc finger protein that regulates neural determination and patterning in Xenopus. *Development* **125**, 2867-2882.
Laudet, V., Hänni, C., Stéhelin, D. and Duterque-Coquillaud, M. (1999). Molecular phylogeny of the ETS gene family. *Oncogene* **18**, 1351-1359.
Le Gallic, L., Sgouras, D., Beal, G., Jr and Mavrothalassitis, G. (1999). Transcriptional repressor ERF is a Ras/mitogen-activated protein kinase target that regulates cellular proliferation. *Mol. Cell. Biol.* **19**, 4121-4133.
Lee, H. C., Tseng, W. A., Lo, F. Y., Liu, T. M. and Tsai, H. J. (2009). FoxD5 mediates anterior-posterior polarity through upstream modulator Fgf signaling during zebrafish somitogenesis. *Dev. Biol.* **336**, 232-245.
Li, R., Pei, H. and Watson, D. K. (2000). Regulation of Ets function by protein – protein interactions. *Oncogene* **19**, 6514-6523.
Lim, L. S., Loh, Y. H., Zhang, W., Li, Y., Chen, X., Wang, Y., Bakre, M., Ng, H. H. and Stanton, L. W. (2007). Zic3 is required for maintenance of pluripotency in embryonic stem cells. *Mol. Biol. Cell* **18**, 1348-1358.
Lim, J. W., Hummert, P., Mills, J. C. and Kroll, K. L. (2011). Geminin cooperates with Polycomb to restrain multi-lineage commitment in the early embryo. *Development* **138**, 33-44.
Lin, C. Y., Su, W. T. and Li, L. T. (2012). Heat-induced antigen retrieval applied in zebrafish: whole-mount in situ immunofluorescence microscopy. *Microsc. Microanal.* **18**, 493-496.
Livak, K. J. and Schmittgen, T. D. (2001). Analysis of relative gene expression data using real-time quantitative PCR and the 2(-Delta Delta C(T)) Method. *Methods* **25**, 402-408.
Maden, M. (2007). Retinoic acid in the development, regeneration and maintenance of the nervous system. *Nat. Rev. Neurosci.* **8**, 755-765.
Marchal, L., Luxardi, G., Thomé, V. and Kodjabachian, L. (2009). BMP inhibition initiates neural induction via FGF signaling and Zic genes. *Proc. Natl. Acad. Sci. USA* **106**, 17437-17442.
Mason, I. (2007). Initiation to end point: the multiple roles of fibroblast growth factors in neural development. *Nat. Rev. Neurosci.* **8**, 583-596.
Mathews, M. B., Bernstein, R. M., Franza, B. R., Jr and Garrels, J. I. (1984). Identity of the proliferating cell nuclear antigen and cyclin. *Nature* **309**, 374-376.
Mavrothalassitis, G. and Ghysdael, J. (2000). Proteins of the ETS family with transcriptional repressor activity. *Oncogene* **19**, 6524-6532.
McGarry, T. J. and Kirschner, M. W. (1998). Geminin, an inhibitor of DNA replication, is degraded during mitosis. *Cell* **93**, 1043-1053.
Merzdorf, C. S. (2007). Emerging roles for zic genes in early development. *Dev. Dyn.* **236**, 922-940.
Miyagi, S., Kato, H. and Okuda, A. (2009). Role of SoxB1 transcription factors in development. *Cell. Mol. Life Sci.* **66**, 3675-3684.
Mizuseki, K., Kishi, M., Matsui, M., Nakanishi, S. and Sasai, Y. (1998). Xenopus Zic-related-1 and Sox-2, two factors induced by chordin, have distinct activities in the initiation of neural induction. *Development* **125**, 579-587.
Moody, S. A. and Je, H. S. (2002). Neural induction, neural fate stabilization, and neural stem cells. *ScientificWorldJournal* **2**, 1147-1166.
Moreno, T. A. and Kintner, C. (2004). Regulation of segmental patterning by retinoic acid signaling during Xenopus somitogenesis. *Dev. Cell* **6**, 205-218.
Morikawa, M., Koinuma, D., Tsutsumi, S., Vasilaki, E., Kanki, Y., Heldin, C. H., Aburatani, H. and Miyazono, K. (2011). ChIP-seq reveals cell type-specific binding patterns of BMP-specific Smads and a novel binding motif. *Nucleic Acids Res.* **39**, 8712-8727.
Muffato, M., Louis, A., Poisnel, C. E. and Roest Crollius, H. (2010). Genomicus: a database and a browser to study gene synteny in modern and ancestral genomes. *Bioinformatics* **26**, 1119-1121.
Nakata, K., Nagai, T., Aruga, J. and Mikoshiba, K. (1997). Xenopus Zic3, a primary regulator both in neural and neural crest development. *Proc. Natl. Acad. Sci. USA* **94**, 11980-11985.
Nakata, K., Nagai, T., Aruga, J. and Mikoshiba, K. (1998). Xenopus Zic family and its role in neural and neural crest development. *Mech. Dev.* **75**, 43-51.
Neilson, K. M., Klein, S. L., Mhaske, P., Mood, K., Daar, I. O. and Moody, S. A. (2012). Specific domains of FoxD4/5 activate and repress neural transcription factor genes to control the progression of immature neural ectoderm to differentiating neural plate. *Dev. Biol.* **365**, 363-375.
Niederreither, K. and Dollé, P. (2008). Retinoic acid in development: towards an integrated view. *Nat. Rev. Genet.* **9**, 541-553.
Nieuwkoop, P. O. and Faber, J. (1967). *A Normal Table of Xenopus Laevis (Daudin): A Systematical and Chronological Survey of The Development From The Fertilized Egg Till The End of Metamorphosis*. Amsterdam: North-Holland Publishing Company.
Oikawa, T. and Yamada, T. (2003). Molecular biology of the Ets family of transcription factors. *Gene* **303**, 11-34.
Papadaki, C., Alexiou, M., Cecena, G., Verykokakis, M., Bilitou, A., Cross, J. C., Oshima, R. G. and Mavrothalassitis, G. (2007). Transcriptional repressor erf determines extraembryonic ectoderm differentiation. *Mol. Cell. Biol.* **27**, 5201-5213.
Papalopulu, N. and Kintner, C. (1996). A posteriorising factor, retinoic acid, reveals that anteroposterior patterning controls the timing of neuronal differentiation in Xenopus neuroectoderm. *Development* **122**, 3409-3418.
Penzel, R., Oschwald, R., Chen, Y., Tacke, L. and Grunz, H. (1997). Characterization and early embryonic expression of a neural specific transcription factor xSOX3 in Xenopus laevis. *Int. J. Dev. Biol.* **41**, 667-677.
Pfaffl, M. W. (2001). A new mathematical model for relative quantification in real-time RT-PCR. *Nucleic Acids Res.* **29**, e45.
Rhinn, M. and Dollé, P. (2012). Retinoic acid signalling during development. *Development* **139**, 843-858.
Rogers, C. D., Moody, S. A. and Casey, E. S. (2009). Neural induction and factors that stabilize a neural fate. *Birth Defects Res. C Embryo Today* **87**, 249-262.
Sawka-Verhelle, D., Escoubet-Lozach, L., Fong, A. L., Hester, K. D., Herzig, S., Lebrun, P. and Glass, C. K. (2004). PE-1/METS, an antiproliferative Ets repressor factor, is induced by CREB-1/CREM-1 during macrophage differentiation. *J. Biol. Chem.* **279**, 17772-17784.
Seo, S., Herr, A., Lim, J. W., Richardson, G. A., Richardson, H. and Kroll, K. L. (2005a). Geminin regulates neuronal differentiation by antagonizing Brg1 activity. *Genes Dev.* **19**, 1723-1734.
Seo, S., Richardson, G. A. and Kroll, K. L. (2005b). The SWI/SNF chromatin remodeling protein Brg1 is required for vertebrate neurogenesis and mediates transactivation of Ngn and NeuroD. *Development* **132**, 105-115.
Sgouras, D. N., Athanasiou, M. A., Beal, G. J., Jr, Fisher, R. J., Blair, D. G. and Mavrothalassitis, G. J. (1995). ERF: an ETS domain protein with strong transcriptional repressor activity, can suppress ets-associated tumorigenesis and is regulated by phosphorylation during cell cycle and mitogenic stimulation. *EMBO J.* **14**, 4781-4793.
Sharpe, C. R. (1992). Two isoforms of retinoic acid receptor alpha expressed during Xenopus development respond to retinoic acid. *Mech. Dev.* **39**, 81-93.
Sharpe, C. R. and Goldstone, K. (1997). Retinoid receptors promote primary neurogenesis in Xenopus. *Development* **124**, 515-523.
Sharpe, C. and Goldstone, K. (2000). The control of Xenopus embryonic primary neurogenesis is mediated by retinoid signalling in the neurectoderm. *Mech. Dev.* **91**, 69-80.
Sharrocks, A. D. (2001). The ETS-domain transcription factor family. *Nat. Rev. Mol. Cell Biol.* **2**, 827-837.
Shiotsugu, J., Katsuyama, Y., Arima, K., Baxter, A., Koide, T., Song, J., Chandraratna, R. A. and Blumberg, B. (2004). Multiple points of interaction between retinoic acid and FGF signaling during embryonic axis formation. *Development* **131**, 2653-2667.
Sive, H. L. and Cheng, P. F. (1991). Retinoic acid perturbs the expression of Xhox.lab genes and alters mesodermal determination in Xenopus laevis. *Genes Dev.* **5**, 1321-1332.
Sive, H. L., Grainger, R. M. and Harland, R. M. (1998). *Early Development of Xenopus Laevis*. Cold Spring Harbor, NY: Cold Spring Harbor Laboratory Press.
Sölter, M., Köster, M., Hollemann, T., Brey, A., Pieler, T. and Knöchel, W. (1999). Characterization of a subfamily of related winged helix genes, XFD-12/12′/12″ (XFLIP), during Xenopus embryogenesis. *Mech. Dev.* **89**, 161-165.
Spella, M., Britz, O., Kotantaki, P., Lygerou, Z., Nishitani, H., Ramsay, R. G., Flordellis, C., Guillemot, F., Mantamadiotis, T. and Taraviras, S. (2007). Licensing regulators Geminin and Cdt1 identify progenitor cells of the mouse CNS in a specific phase of the cell cycle. *Neuroscience* **147**, 373-387.
Sullivan, S. A., Akers, L. and Moody, S. A. (2001). foxD5a, a Xenopus winged helix gene, maintains an immature neural ectoderm via transcriptional repression that is dependent on the C-terminal domain. *Dev. Biol.* **232**, 439-457.
Tabar, V., Panagiotakos, G., Greenberg, E. D., Chan, B. K., Sadelain, M., Gutin, P. H. and Studer, L. (2005). Migration and differentiation of neural precursors derived from human embryonic stem cells in the rat brain. *Nat. Biotechnol.* **23**, 601-606.
Tabb, M. M., Kholodovych, V., Grun, F., Zhou, C., Welsh, W. J. and Blumberg, B. (2004). Highly chlorinated PCBs inhibit the human xenobiotic response mediated by the steroid and xenobiotic receptor (SXR). *Environ. Health Perspect.* **112**, 163-169.
Tropepe, V., Li, S., Dickinson, A., Gamse, J. T. and Sive, H. L. (2006). Identification of a BMP inhibitor-responsive promoter module required for expression of the early neural gene zic1. *Dev. Biol.* **289**, 517-529.
Verykokakis, M., Papadaki, C., Vorgia, E., Le Gallic, L. and Mavrothalassitis, G. (2007). The RAS-dependent ERF control of cell proliferation and differentiation is mediated by c-Myc repression. *J. Biol. Chem.* **282**, 30285-30294.

Wagner, L. E., 2nd, Li, W. H., Joseph, S. K. and Yule, D. I. (2004). Functional consequences of phosphomimetic mutations at key cAMP-dependent protein kinase phosphorylation sites in the type 1 inositol 1,4,5-trisphosphate receptor. *J. Biol. Chem.* **279**, 46242-46252.
Wasylyk, B., Hagman, J. and Gutierrez-Hartmann, A. (1998). Ets transcription factors: nuclear effectors of the Ras-MAP-kinase signaling pathway. *Trends Biochem. Sci.* **23**, 213-216.
Wegner, M. and Stolt, C. C. (2005). From stem cells to neurons and glia: a Soxist's view of neural development. *Trends Neurosci.* **28**, 583-588.
Wills, A. E., Choi, V. M., Bennett, M. J., Khokha, M. K. and Harland, R. M. (2010). BMP antagonists and FGF signaling contribute to different domains of the neural plate in Xenopus. *Dev. Biol.* **337**, 335-350.
Wilson, P. A. and Hemmati-Brivanlou, A. (1995). Induction of epidermis and inhibition of neural fate by Bmp-4. *Nature* **376**, 331-333.
Wullimann, M. F., Rink, E., Vernier, P. and Schlosser, G. (2005). Secondary neurogenesis in the brain of the African clawed frog, Xenopus laevis, as revealed by PCNA, Delta-1, Neurogenin-related-1, and NeuroD expression. *J. Comp. Neurol.* **489**, 387-402.
Yan, B., Neilson, K. M. and Moody, S. A. (2009). foxD5 plays a critical upstream role in regulating neural ectodermal fate and the onset of neural differentiation. *Dev. Biol.* **329**, 80-95.
Yan, B., Neilson, K. M. and Moody, S. A. (2010). Microarray identification of novel downstream targets of FoxD4L1/D5, a critical component of the neural ectodermal transcriptional network. *Dev. Dyn.* **239**, 3467-3480.

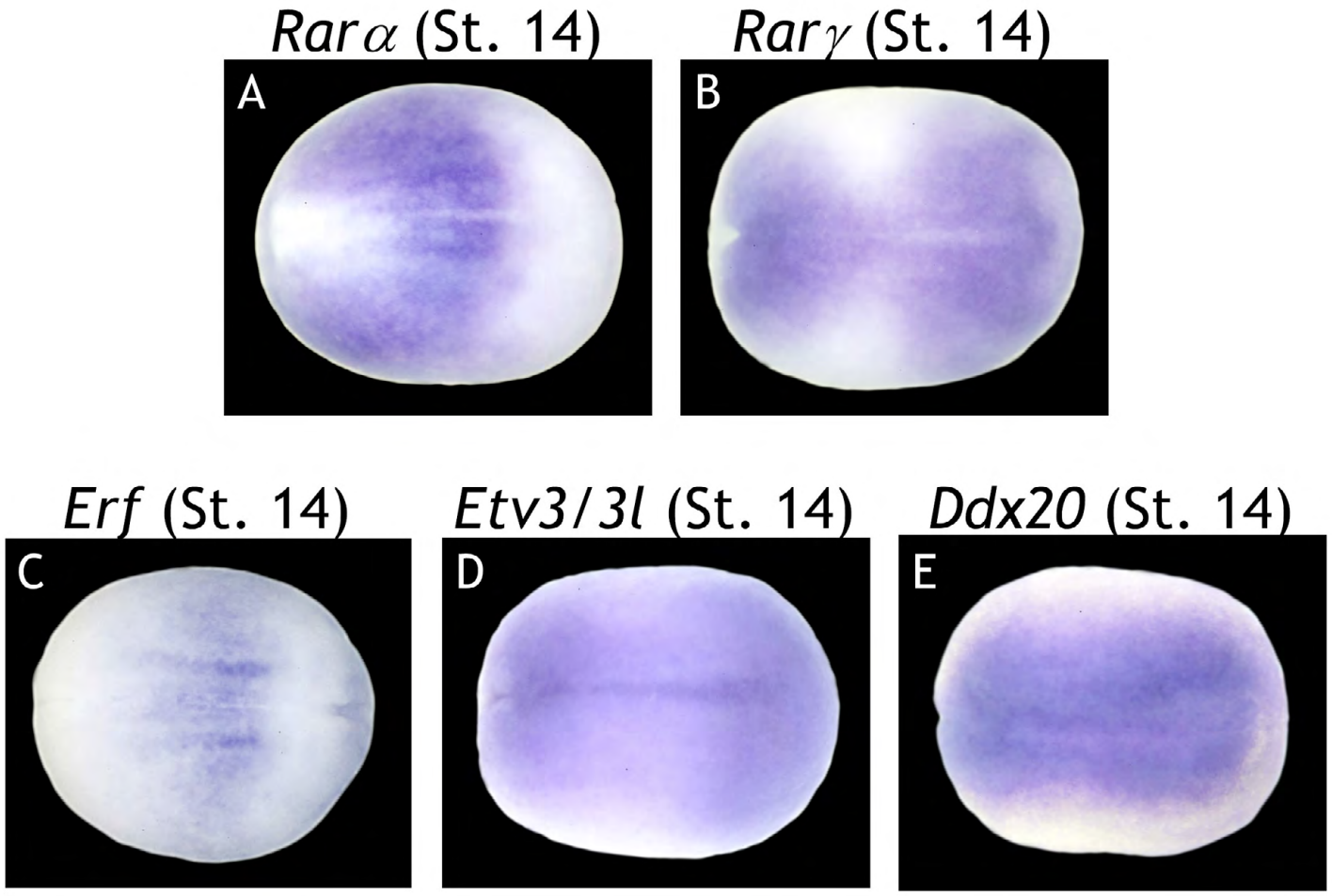

Fig. S1. Qualitative expression of *Rarα*, *Rarγ*, *Erf*, *Etv3/3l* and *Ddx20* at stage 14. (**A-E**) Whole-mount *in situ* hybridization of *Rarα* (A), *Rarγ* (B), *Erf* (C), *Etv3/3l* (D) and *Ddx20* (E) gene expression at Nieuwkoop and Faber stage 14. Dorsal views are shown with anterior towards the right.

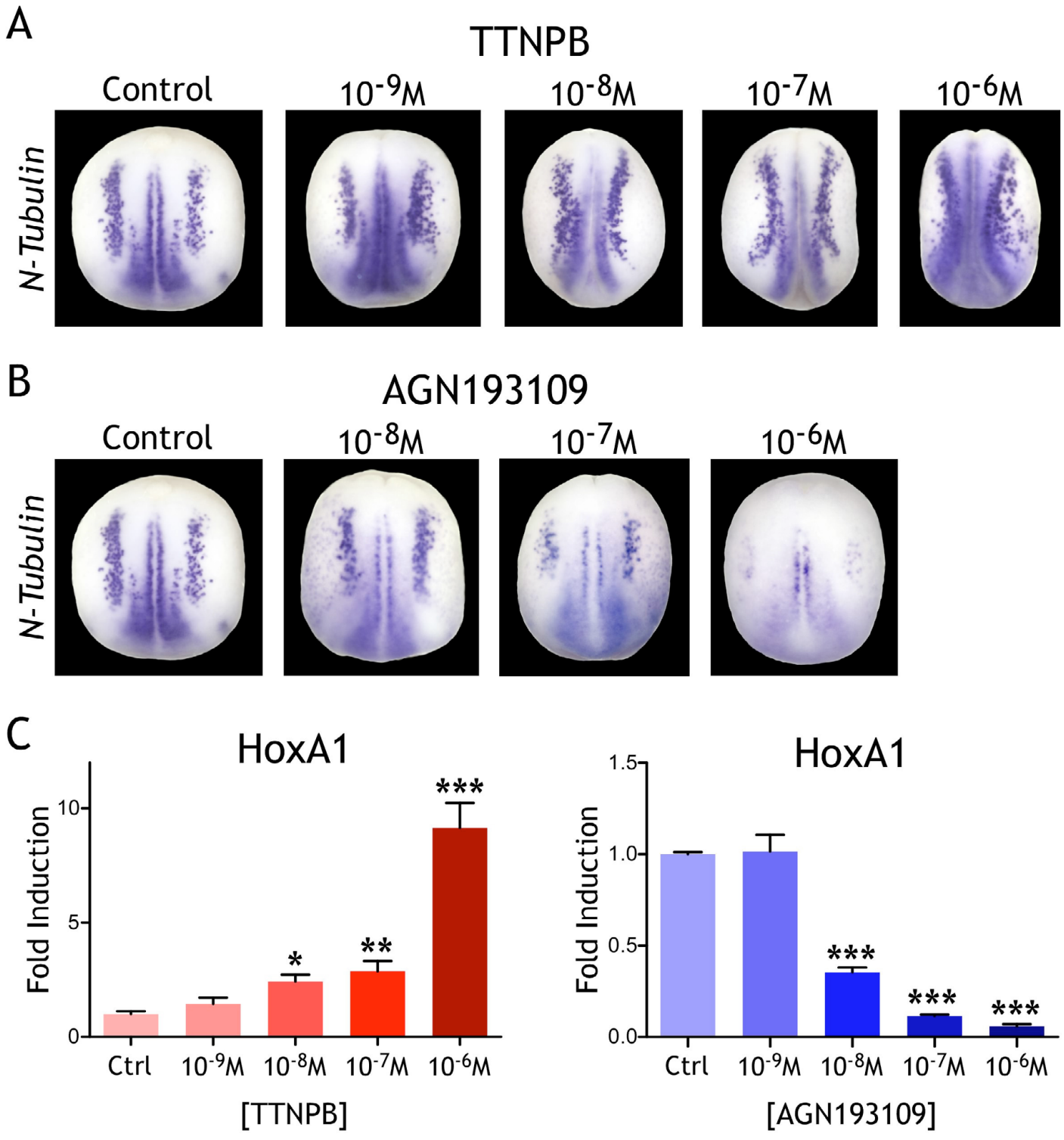

Fig. S2. Dose response of TTNPB and AGN193109. (**A**,**B**) Whole-mount *in situ* hybridization from whole embryos treated at stage 7/8 with 1 nM to 1 µM TTNPB, 10 nM to 1 µM AGN193109 or control vehicle (0.1% ethanol). Dorsal *N-tubulin* expression is increased with TTNPB treatment at doses as low as 10^{-9} M, compared with control. AGN193109 causes loss of *N-tubulin* expression at doses as low as 10^{-7} M. (**C**) QPCR showing *HoxA1* expression in embryos treated at stage 7/8 with 1 nM to 1 µM TTNPB, 1 nM to 1 µM AGN193109 or vehicle (0.1% ethanol). The *y*-axis represents $2^{-\Delta\Delta Ct}$ values normalized to *Histone H4* and expressed as fold induction relative to control. *HoxA1* is induced by TTNPB at doses as low as 10^{-9} M and repressed by AGN193109 at doses as low as 10^{-8} M. Asterisks represent statistical significance compared with control (*$P \leq 0.05$, **$P \leq 0.01$, ***$P \leq 0.001$).

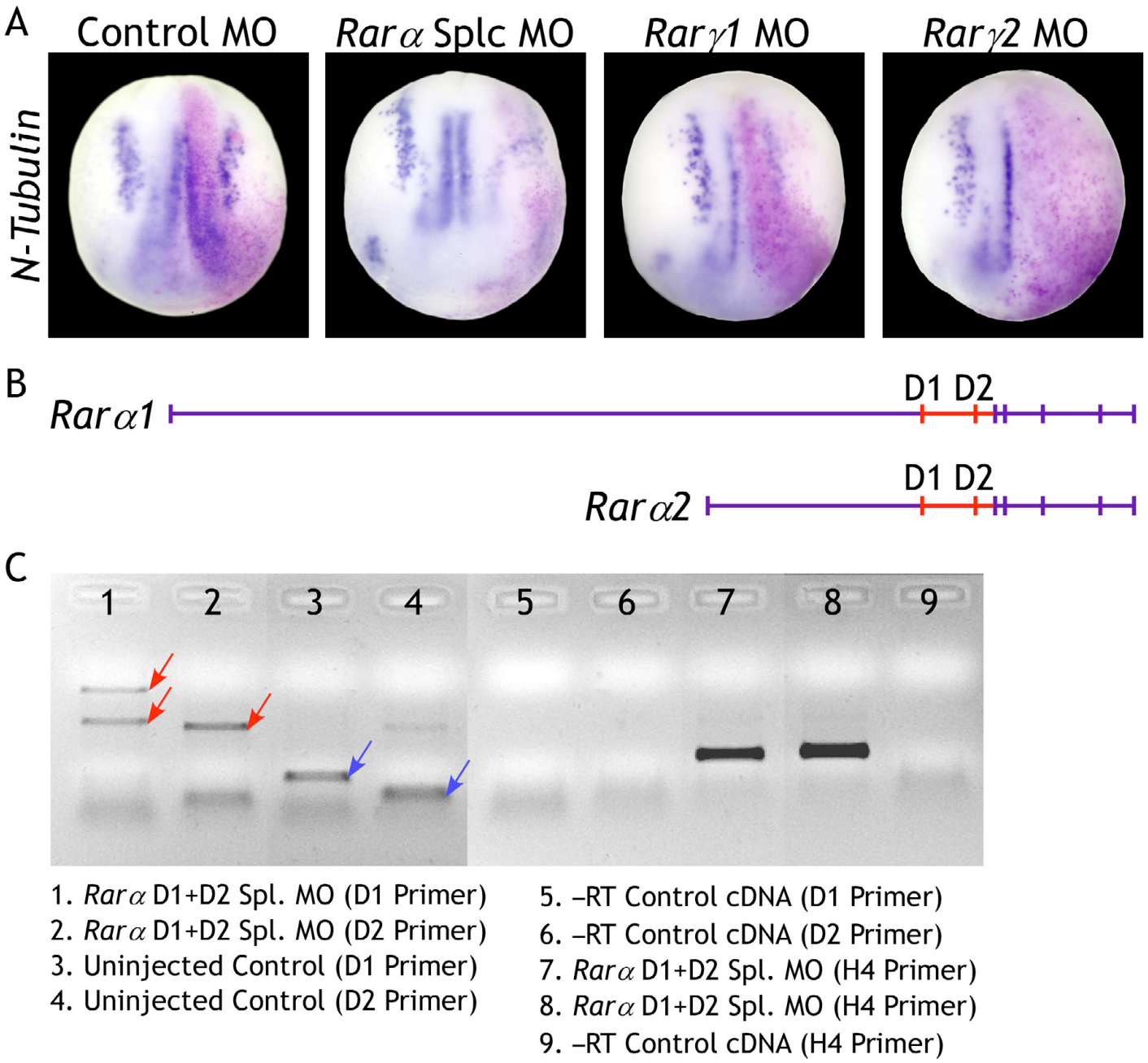

Fig. S3. Specificity of *Rarα* and *Rarγ* MO phenotypes. All embryos were injected unilaterally at the two- or four-cell stage. The injected side is indicated by the magenta *β-gal* mRNA lineage tracer. For *Rarα*, we employed two additional splice MOs that target two exon-intron splice donor boundaries of *Rarα* (D1, splice donor 1; D2, splice donor 2). For *Rarγ*, we used two different translation-inhibiting MOs, one targeting *Rarγ1* and the other *Rarγ2*. (**A**) Knockdown of *N-tubulin* was observed in embryos injected with 10 ng *Rarα* splice MO D1 + 20 ng *Rarα* splice MO D2 (14/18 embryos), and in embryos injected with 3.75 ng *Rarγ1* MO (17/17) or 3.75 ng *Rarγ2* MO (7/11). Embryos are shown in dorsal view with anterior at the bottom, at stage 14. (**B**) The exon-intron borders targeted by the two *Rarα* splice MOs. The splice MOs target both *Rarα1* and *Rarα2*. (**C**) PCR and gel electrophoresis of cDNA from uninjected embryos or embryos bilaterally injected with *Rarα* splice MOs. Spliced mRNAs are indicated by blue arrows. Both *Rarα* splice MOs (D1 and D2) result in unspliced PCR products (indicated by red arrows), whereas spliced PCR products are diminished in these lanes. RT, minus reverse transcriptase control (cDNA synthesis of pooled RNA without reverse transcriptase enzyme); H4, *Histone H4* (reference gene).

A

```
RARγ1      tagaacaaggcaATGGCAAACAGC
RARγ2      cccaaaATGTATGACTGCATGGAA
RARα1      gagggagtagaagtgcgtttggagc
RARα2.1    actctATGGTCAGTTTGGATTTCAG
RARα2.2    cacacacactcaccttcctttggat
```

B

```
RARγ1      atggatttatcactgaataactaaggaagacattggtacccaaggaagattccaagacaactact
RARγ2      cgga-----------------------------------aggtgccaatctcagtctgctacc
RARα1      cagtt----------------------------------ggattaagtgccaggccgacgttt
RARα2.1    tgggaaatctc----------------cagtggttctgctgtggggacattcctcctgagcccca
RARα2.2    ctttattatta----------------ttattattat----tattattcccctaattcaaccccc
                                                    .       *       .*

RARγ1      gg--------------------ctagcactaagtaagagactgagct------------------
RARγ2      aga-gcccacactgctgctttcccaccctcttctgaaaacttcagtg--cctgcttacccgctcc
RARα1      gggggtgagccccccccgacccccacaaatggagaagctgaggg----agtagaagtgcgtt
RARα2.1    aagcctttcgctccggatcatccccccgttacccagactgctcggtt-----------------
RARα2.2    ccccacacacacactcaccttcctttggatatatgctgactttgggg-----------------
                              *       :   .      * .*

RARγ1      --agaacaaggcaATGGCAAACAGCAGCAAGGAGCGCCTCTGTGGGGCTGGGGCTCCTCTGGGA
RARγ2      CTGTACACCCAAAATGTATGACTGCATGGAATCCTTCCCTTTGATGCCTCGGCCGCTCTATGAC
RARα1      tggagctgaggcaATGAGCAGTAAGGACAACACTTGCCCCCCTCCTGGGCCCGGCCACATCAAT
RARα2.1    ------ccactctATGGTCAGTTTGGATTTCAGTAGAATGTACGAGAATGTGGACGTTCCTGCT
RARα2.2    --gggcctttaggATGTATGAGAATGTGGACGTCAGCCCCACTCACTACCACATGATGGATTTC
             .       . .***   .. :. .  .*
```

Fig. S4. Uniqueness of *Rar* MO target sequence. (**A**) Nucleotide sequence targeted by MOs with protein-coding sequence in capitals. (**B**) MAFFT alignment of relevant regions of the 5'UTR and variable 5' coding of RAR isoforms in *Xenopus laevis*, demonstrating no sequence similarity and that all MOs are specific for the receptor subtype or isoform they are directed against.

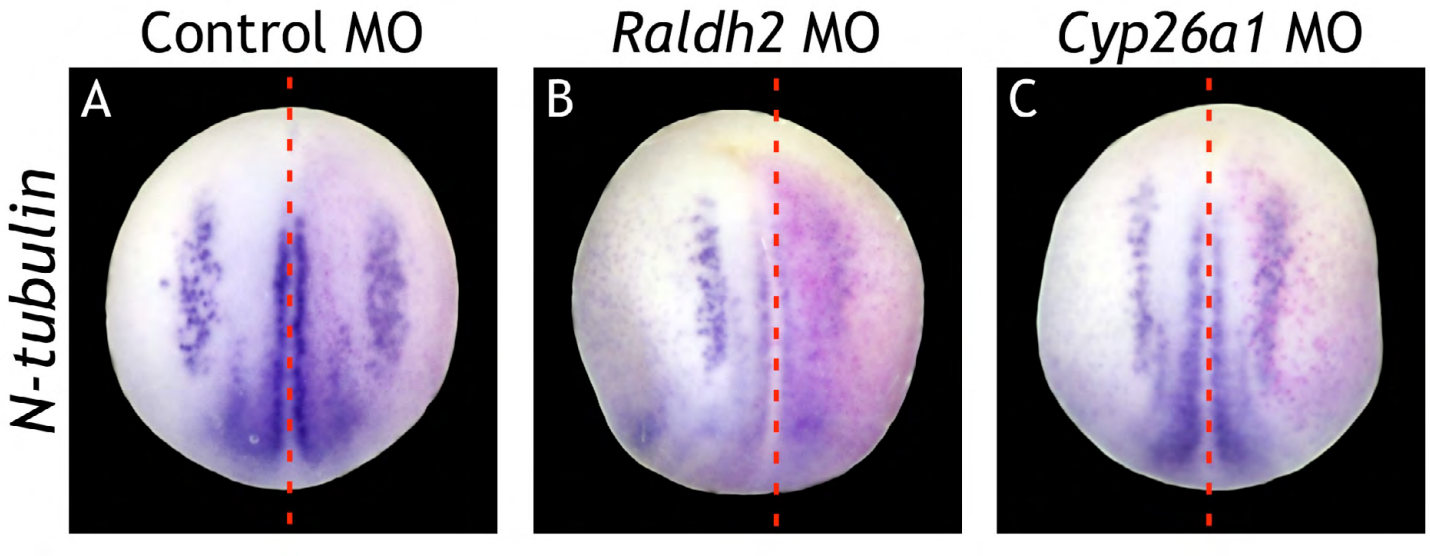

Fig. S5. *N-tubulin* is RA responsive and requires RALDH2 for its expression, whereas knockdown of *Cyp26a1* increases *N-tubulin* expression. All embryos were injected unilaterally at the two- or four-cell stage. The injected side is indicated by the magenta *β-gal* mRNA lineage tracer. (**A**) Control expression of *N-tubulin*. (**B**) 20 ng *Raldh2* MO reduced expression of *N-tubulin* (14/31 embryos), confirming the requirement for RA signaling in primary neurogenesis. (**C**) 20 ng *Cyp26a1* MO increased expression of *N-tubulin* (12/28 embryos) presumably by increasing embryonic RA levels. All embryos are shown in dorsal view with anterior at the bottom, at stage 14.

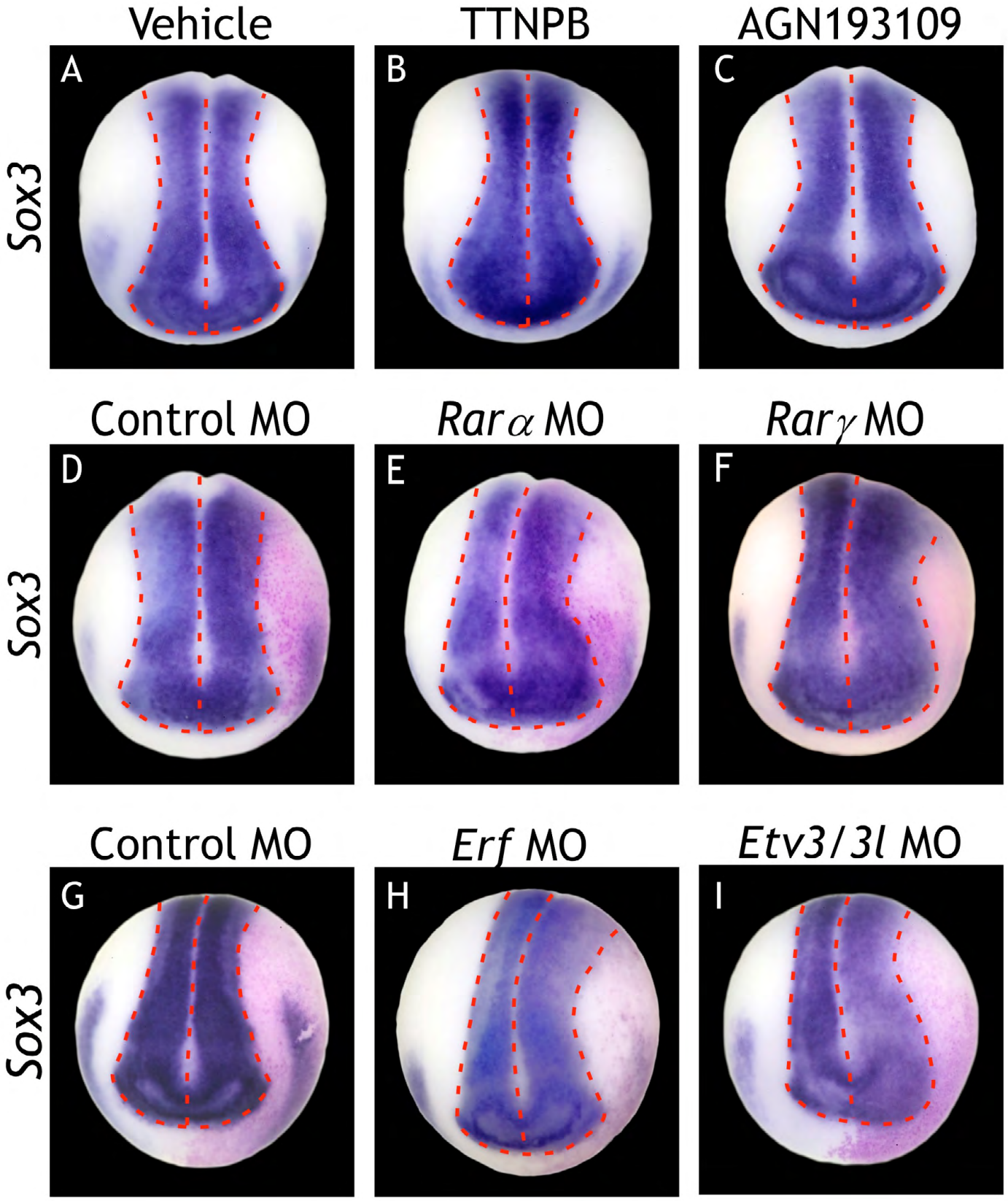

Fig. S6. *Sox3* is modulated by RAR signaling; ERF or ETV3/3L knockdown expand expression of *Sox3*. (**A-C**) Whole-mount *in situ* hybridization from whole embryos treated at stage 7/8 with 1 µM TTNPB, 1 µM AGN193109 or control vehicle (0.1% ethanol). *Sox3* expression is slightly narrowed in the anterior domain with TTNPB treatment (17/19) compared with control. AGN193109 (a RAR-specific antagonist) causes anterior expansion of *Sox3* (15/22). (**D-I**) All embryos were injected unilaterally at the two- or four-cell stage. The injected side is indicated by the magenta *β-gal* mRNA lineage tracer. (**D**,**G**) Control expression of *Sox3*. (**E**) 3.3 ng *Rarα1* MO + 3.3 ng *Rarα2.1* MO + 3.3 ng *Rarα2.2* MO expanded expression of *Sox3* (13/15 embryos). (**F**) 3.75 ng *Rarγ1* MO + 3.75 *Rarγ2* MO expanded expression of *Sox3* (21/22). (**H**,**I**) 10 ng Erf MO expanded *Sox3* expression (8/14) and 20 ng *Etv3/3l* MO expanded *Sox3* expression (11/17). All embryos are shown in dorsal view with anterior at the bottom, at stage 14.

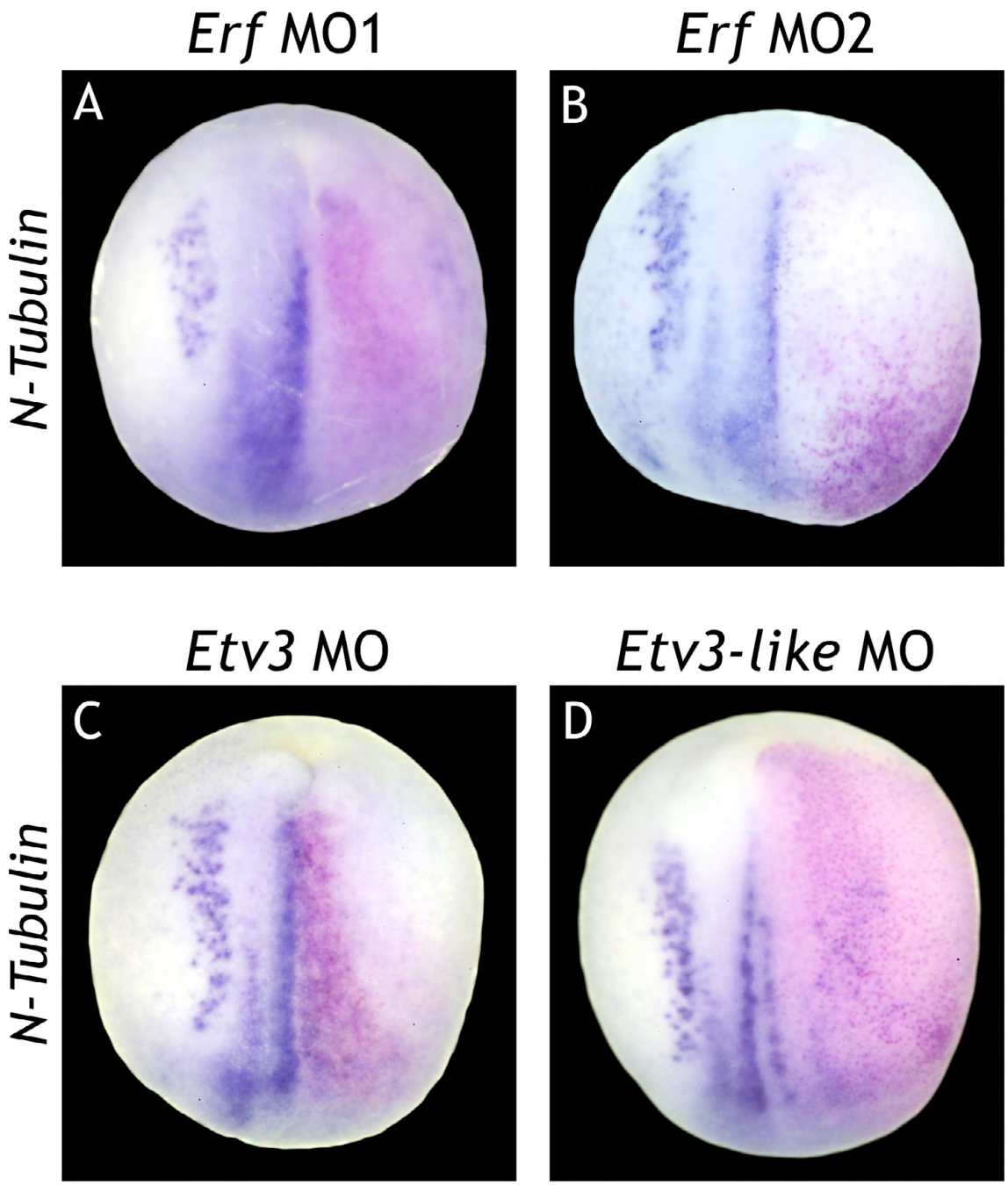

Fig. S7. Specificity of *Erf*-MO and *Etv3/3l*-MO phenotypes. All embryos were injected unilaterally at the two- or four-cell stage. The injected side is indicated by the magenta *β-gal* mRNA lineage tracer. Knockdown or knockout of *N-tubulin* was observed in embryos injected with (**A**) 10 ng *Erf* AUG MO #1 (30/35 embryos), (**B**) 10 ng *Erf* AUG MO #2 (18/19), (**C**) 20 ng *Etv3* AUG MO (10/11) and (**D**) 20 ng *Etv3l* AUG MO (16/21). Embryos are shown in dorsal view with anterior at the bottom, at stage 14.

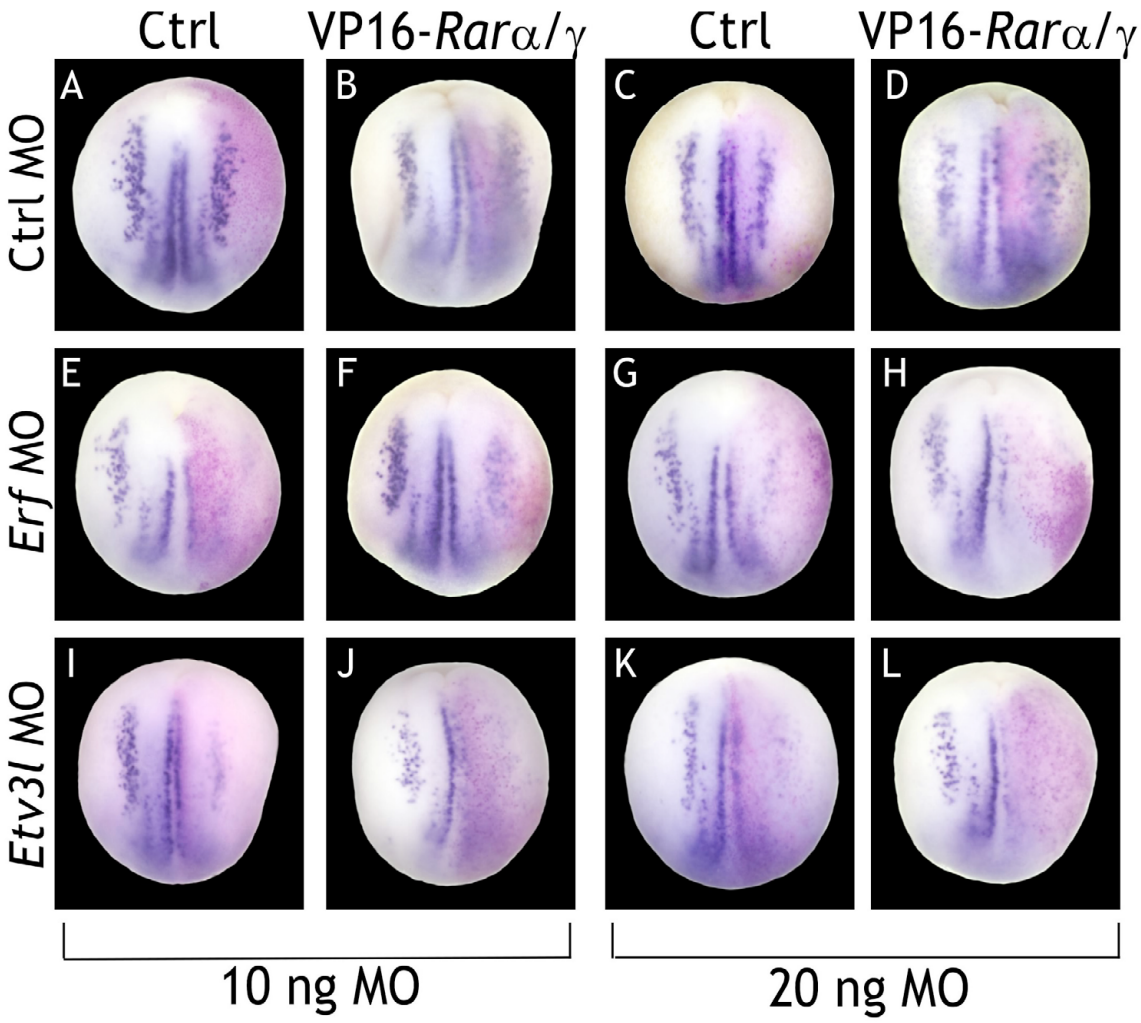

M

	Injection Combination	NT	LT	NC	ExN	EcN	Total
A	10 ng Ctrl MO + 100 pg *mCherry* mRNA	0	4	34	0	0	38
B	10 ng Ctrl MO + 100 pg VP16-*Rar*α/γ mRNA	0	11	2	11	12	36
C	20 ng Ctrl MO + 100 pg *mCherry* mRNA	0	13	30	0	6	49
D	20 ng Ctrl MO + 100 pg VP16-*Rar*α/γ mRNA	0	10	2	5	19	36
E	10 ng *Erf* MO + 100 pg *mCherry* mRNA	15	14	0	1	0	30
F	10 ng *Erf* MO + 100 pg VP16-*Rar*α/γ mRNA	7	6	4	3	5	25
G	20 ng *Erf* MO + 100 pg *mCherry* mRNA	17	6	1	0	0	24
H	20 ng *Erf* MO + 100 pg VP16-*Rar*α/γ mRNA	29	3	0	1	0	33
I	10 ng *Etv3l* MO + 100 pg *mCherry* mRNA	4	20	9	0	0	33
J	10 ng *Etv3l* MO + 100 pg VP16-*Rar*α/γ mRNA	29	11	0	0	0	40
K	20 ng *Etv3l* MO + 100 pg *mCherry* mRNA	21	6	0	0	0	27
L	20 ng *Etv3l* MO + 100 pg VP16-*Rar*α/γ mRNA	35	5	0	0	0	40

NT = no tubulin; LT = low tubulin; NC = no change; ExN = Extra Neurons; EcN = Ectopic Neurons

Fig. S8. ERF or ETV3L knockdown rescues the extra/ectopic neuron phenotype generated by VP16-*Rarα/γ* mRNA. All embryos were injected unilaterally at the two- or four-cell stage. The injected side is indicated by the magenta *β-gal* mRNA lineage tracer. (**A**,**C**) 10 ng or 20 ng control MO + 0.1 ng *mCherry* (control) mRNA does not change expression of *N-tubulin*. (**B**,**D**) 10 ng or 20 ng control MO + 0.1 ng VP16- *Rarα/γ* mRNA results in extra and/or ectopic neurons. (**E-H**) 10 ng *Erf* MO partially rescues (68%) and 20 ng *Erf* MO completely rescues (97%) VP16-*Rarα/γ* mRNA extra/ectopic neuron phenotype. (**I-L**) 10 ng or 20 ng *Etv3l* MO completely rescues (100%) VP16-*Rarα/γ* mRNA extra/ectopic neuron phenotype. Embryos are shown in dorsal view with anterior at the bottom, at stage 14. (**M**) Detailed scoring of embryos represented in A-L.

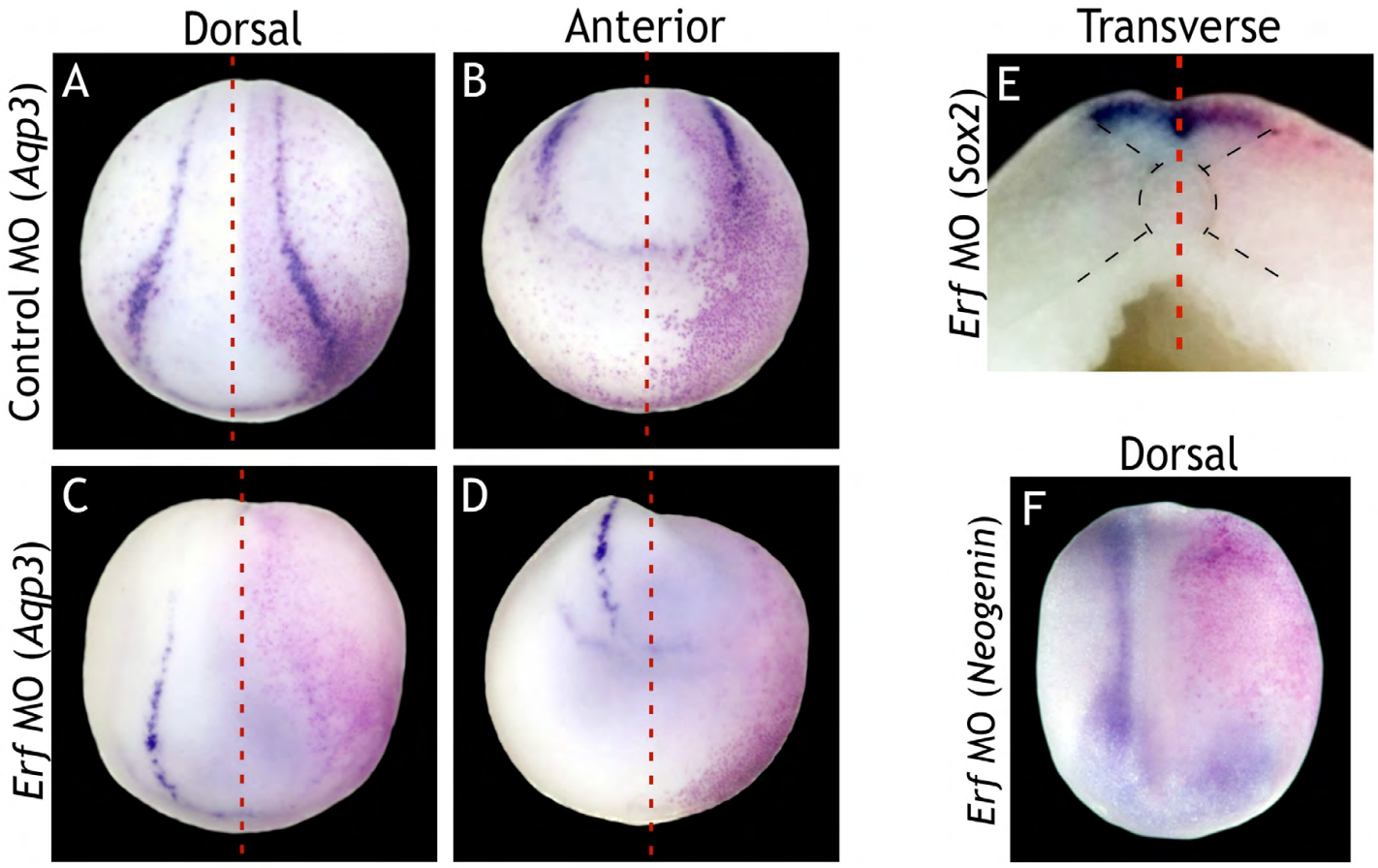

Fig. S9. ERF knockdown inhibits neural fold elevation. All embryos were injected unilaterally at the two- or four-cell stage. The injected side is indicated by the magenta *β-gal* mRNA lineage tracer. (**A**,**B**) Dorsal (A) and anterior (B) views of 10 ng control MO, stained for *Aqp3* at stage 14. (**C**,**D**) Dorsal (C) and anterior (D) views of 10 ng *Erf* MO, which resulted in a flattening of neural folds and significant reduction of *Aqp3* at stage 14 (7/7 embryos). The flattening of the neural folds was observed in 60-70% of embryos in all experiments using *Erf* MO. (**E**) A transverse section of a stage 22 embryo injected with 10 ng *Erf* MO reveals relatively normal neural structure, as revealed by *Sox2* expression. (**F**) Dorsal view of 10 ng *Erf* MO which resulted in loss of *Neogenin* (7/9 embryos) at stage 14.

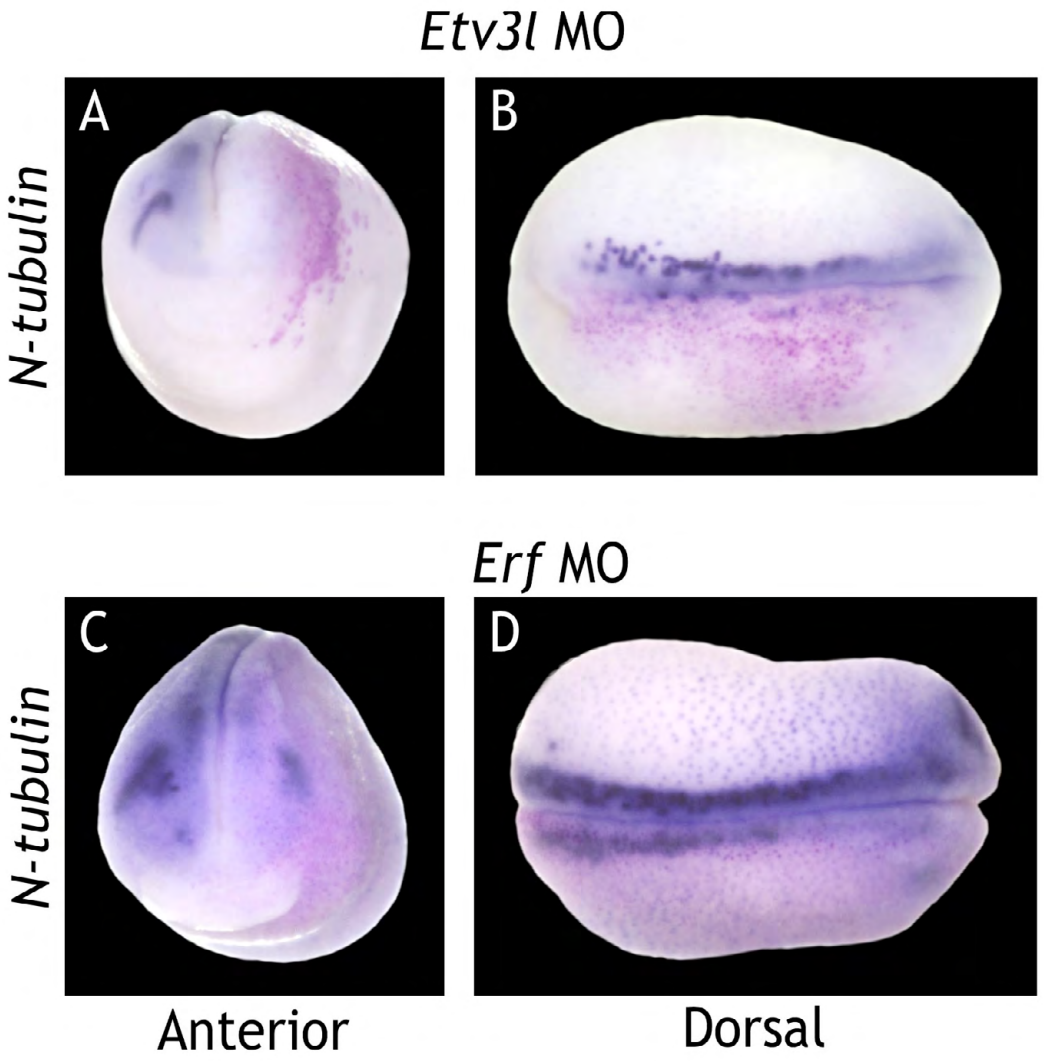

Fig. S10. ERF or ETV3L knockdown causes a decrease or loss of *N-tubulin* in stage 22 embryos. All embryos were injected unilaterally at the two- or four-cell stage. The injected side is indicated by the magenta *β-gal* mRNA lineage tracer. (**A**,**B**) Anterior (A) and dorsal (B) views of 20 ng *Etv3l* MO, which resulted in loss of *N-tubulin* expression at stage 22 (25/26 embryos). (**C**,**D**) Anterior (C) and dorsal (D) views of 10 ng *Erf* MO, which resulted in decreased *N-tubulin* expression at stage 22 (16/32 embryos).

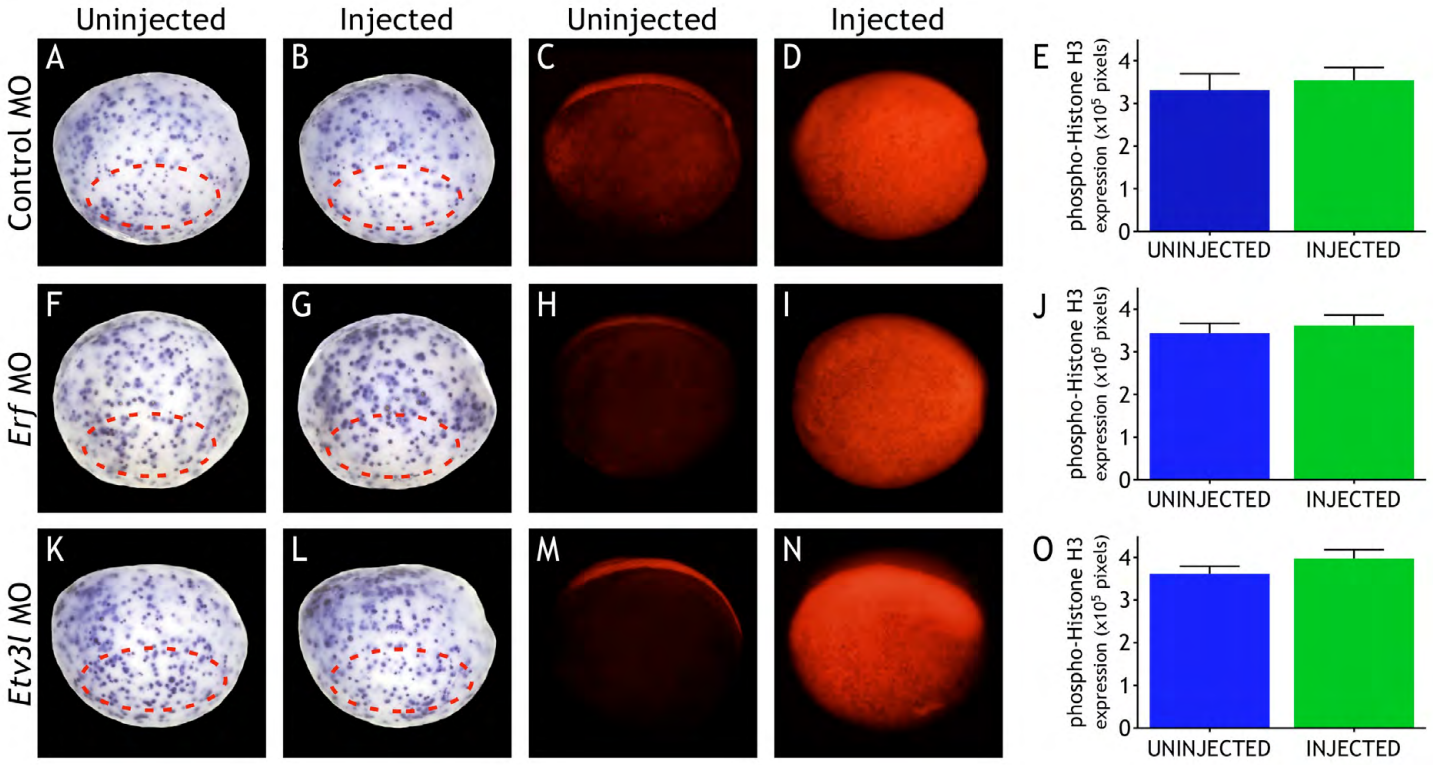

Fig. S11. ERF or ETV3L knockdown does not change proliferation outside of the neural plate. Embryos were injected unilaterally at the 2- or 4-cell stage. The injected side is indicated by the red fluorescent lineage tracer. (**A-D**,**F-I**,**K-N**) Representative photographs in bright-field (A,B,F,G,K,L) and fluorescence (C,D,H,I,M,N) are shown. (A-D) Photographs of the same stage 14 embryo, in lateral view, with B and D flipped horizontally from A and C, such that the anterior of the embryo is always on the left. The same is true for F-I and K-N. (**E**,**J**,**O**) Quantitation of phospho-*Histone H3* staining for all embryos in the experiment is provided in bar graphs. (A-O) Embryos injected with 10 ng control MO (A-E), 10 ng *Erf* MO (F-J) or 20 ng *Etv3l* MO (K-O) showed no significant difference in phospho-*Histone H3* staining on the injected versus the uninjected side (Ctrl MO, n=21, P=0.4654; *Erf* MO, n=39, P=0.5329; *Etv3l* MO, n=47, P=0.2256).

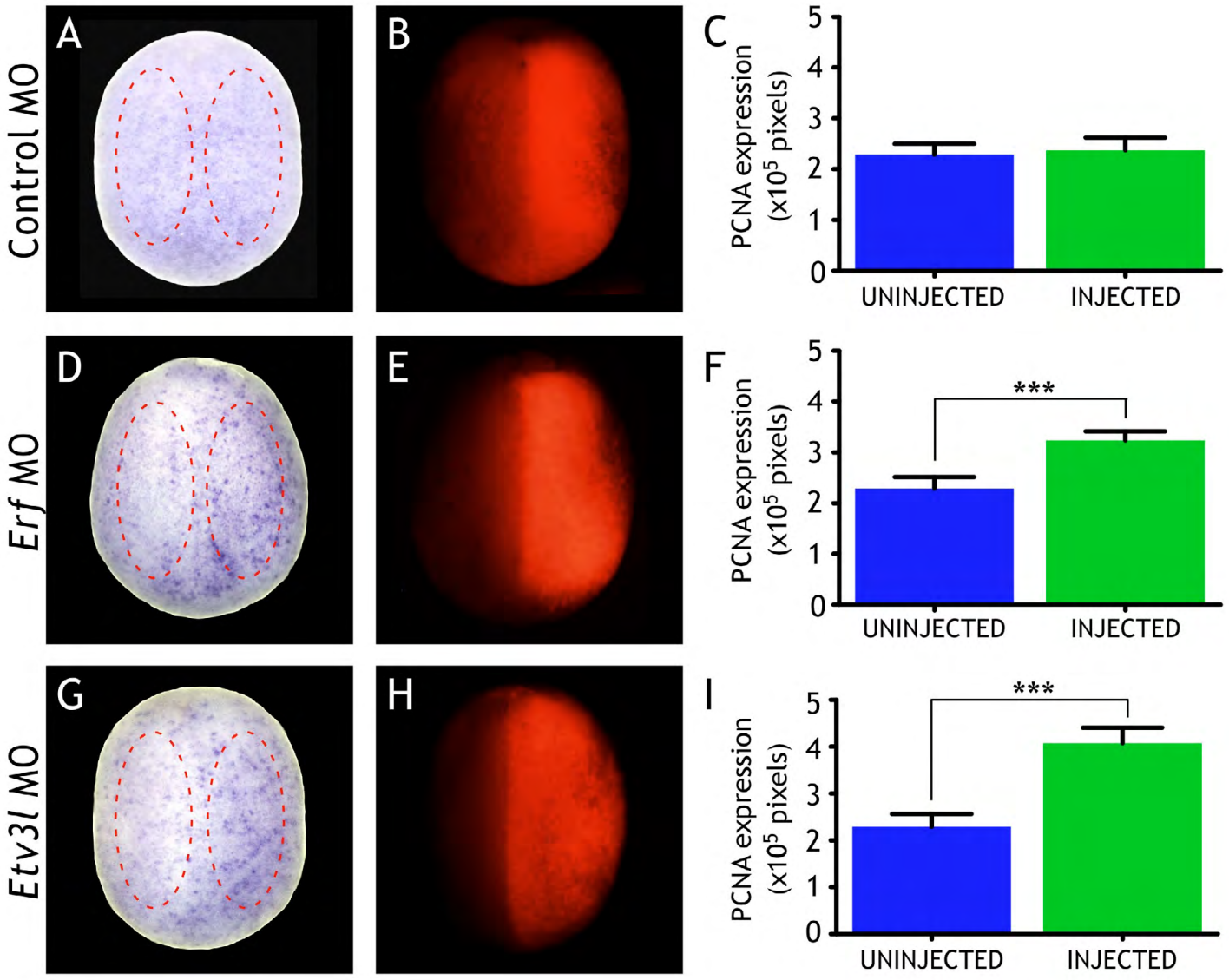

Fig. S12. ERF or ETV3L knockdown increases proliferation in the neural plate. Embryos were injected unilaterally at the 2- or 4-cell stage. (A,B,D,E,G,H) The injected side is indicated by the red fluorescent lineage tracer. Representative photographs in brightfield (A,D,G) and fluorescence (B,E,H) are shown. (C,F,I) Quantitation of PCNA staining for all embryos in the experiment is provided in bar graphs. Embryos are shown in dorsal view at stage 14; anterior is at the bottom. (**A-C**) Embryos injected with 10 ng control MO showed no significant difference in the number of PCNA nuclei on the injected versus the uninjected side (n=41; P=0.776). (**D-F**) Embryos injected with 10 ng *Erf* MO showed an increased number of PCNA nuclei on the injected side (n=45; P=0.0009). (**G-I**) Embryos injected with 10 ng *Etv3l* MO showed an increased number of PCNA nuclei on the injected side (n=46; P=0.0009).

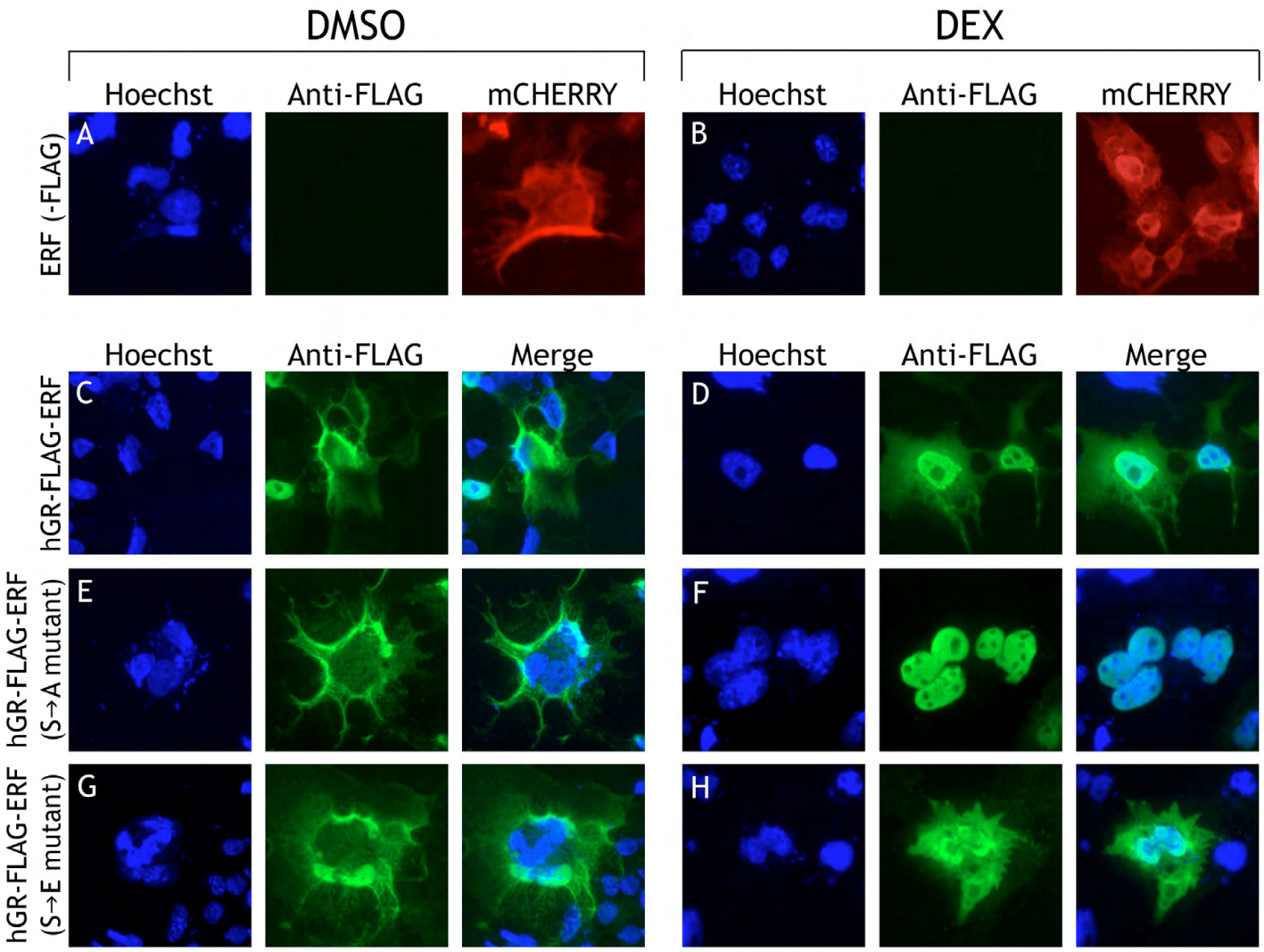

Fig. S13. Subcellular localization of hGR-ERF. COS-7 cells were co-transfected with *mCherry* and either *Erf* (no FLAG), FLAG-*hGR-Erf* (WT), FLAG-*hGR-Erf* ($S^{246,251}\rightarrow A^{246,251}$) or FLAG-*hGR-Erf* ($S^{246,251}\rightarrow E^{246,251}$), then treated with 1 μM dexamethasone (DEX) or 0.01% DMSO. (**A**,**B**) Negative control with *Erf* (no FLAG); transfected cells are indicated by mCHERRY fluorescence. (**C**,**E**,**G**) All FLAG-hGR-ERF proteins are found mostly in the cytoplasm when cells were treated with DMSO. (**D**) Dexamethasone-treated FLAG-hGR-ERF (WT) is located in the cytoplasm and the nucleus. (**F**) Dexamethasone-treated FLAG-hGR-ERF ($S^{246,251}\rightarrow A^{246,251}$) is located exclusively in the nucleus (**H**) Dexamethasone-treated FLAG-hGR-ERF ($S^{246,251}\rightarrow E^{246,251}$) is located in the cytoplasm and the nucleus.

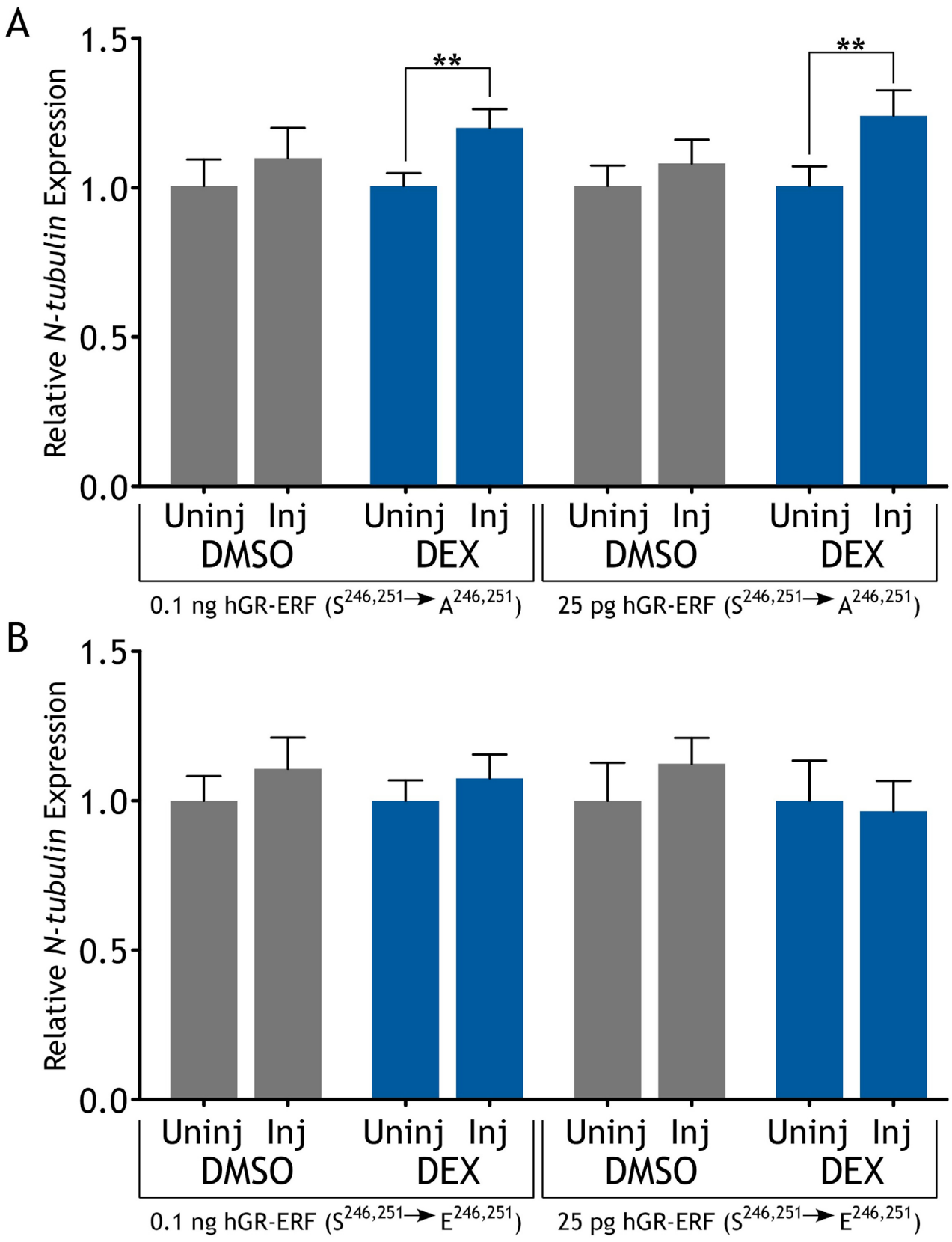

Fig. S14. ERF gain of function increases primary neurons. Embryos were injected unilaterally at the 2- or 4-cell stage, then treated with 10 μM dexamethasone (DEX) or 0.1% DMSO vehicle at stage 11. Quantitation of *N-tubulin* expression at stage 14 is shown. (**A**) Embryos injected with 0.1 ng or 25 pg *hGR-Erf* ($S^{246,251}$→$A^{246,251}$) mRNA and treated with dexamethasone showed a significant increase in neurons on the injected side (0.1 ng, *n*=29, *P*=0.0073; 25 pg, *n*=23, *P*=0.0049). DMSO-treated embryos showed no significant difference in neurons (0.1 ng, *n*=22, *P*=0.4170; 25 pg, *n*=22, *P*=0.2558) (**B**) Embryos injected with 0.1 ng or 25 pg *hGR-Erf* ($S^{246,251}$ → $E^{246,251}$) mRNA showed no significant difference in neurons on the injected versus the uninjected side in dexamethasone-treated (0.1 ng, *n*=22, *P*=0.2055; 25 pg, *n*=13, *P*=0.7354) or DMSO-treated embryos (0.1 ng, *n*=16, *P*=0.6233; 25 pg, *n*=10, *P*=0.1309).

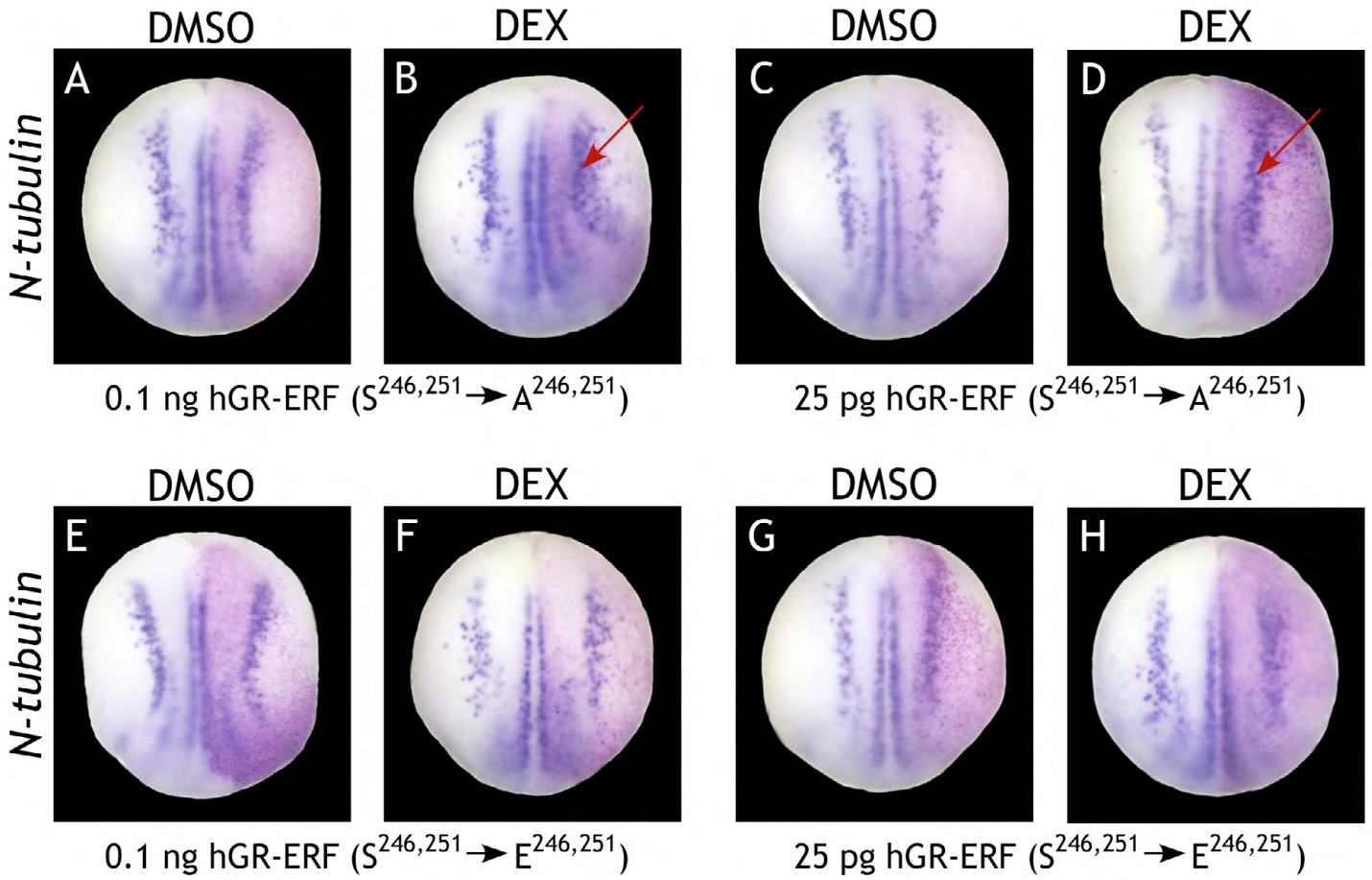

Fig. S15. ERF gain of function increases primary neurons. Embryos corresponding to data provided in Fig. 9. (**A**) DMSO-treated or (**B**) dexamethasone-treated embryos injected with 0.1 ng *hGR-Erf* ($S^{246,251}\rightarrow A^{246,251}$) mRNA. (**C**) DMSO-treated or (**D**) dexamethasone-treated embryos injected with 25 pg *hGR-Erf* ($S^{246,251}\rightarrow A^{246,251}$) mRNA. (**E**) DMSO-treated or (**F**) dexamethasone-treated embryos injected with 0.1 ng *hGR-Erf* ($S^{246,251}\rightarrow E^{246,251}$) mRNA. (**G**) DMSO-treated or (**H**) dexamethasone-treated embryos injected with 25 pg *hGR-Erf* ($S^{246,251}\rightarrow E^{246,251}$) mRNA. The red arrows indicate the increase in *N-tubulin* expression. All embryos are shown in dorsal view with anterior at the bottom, at stage 14.

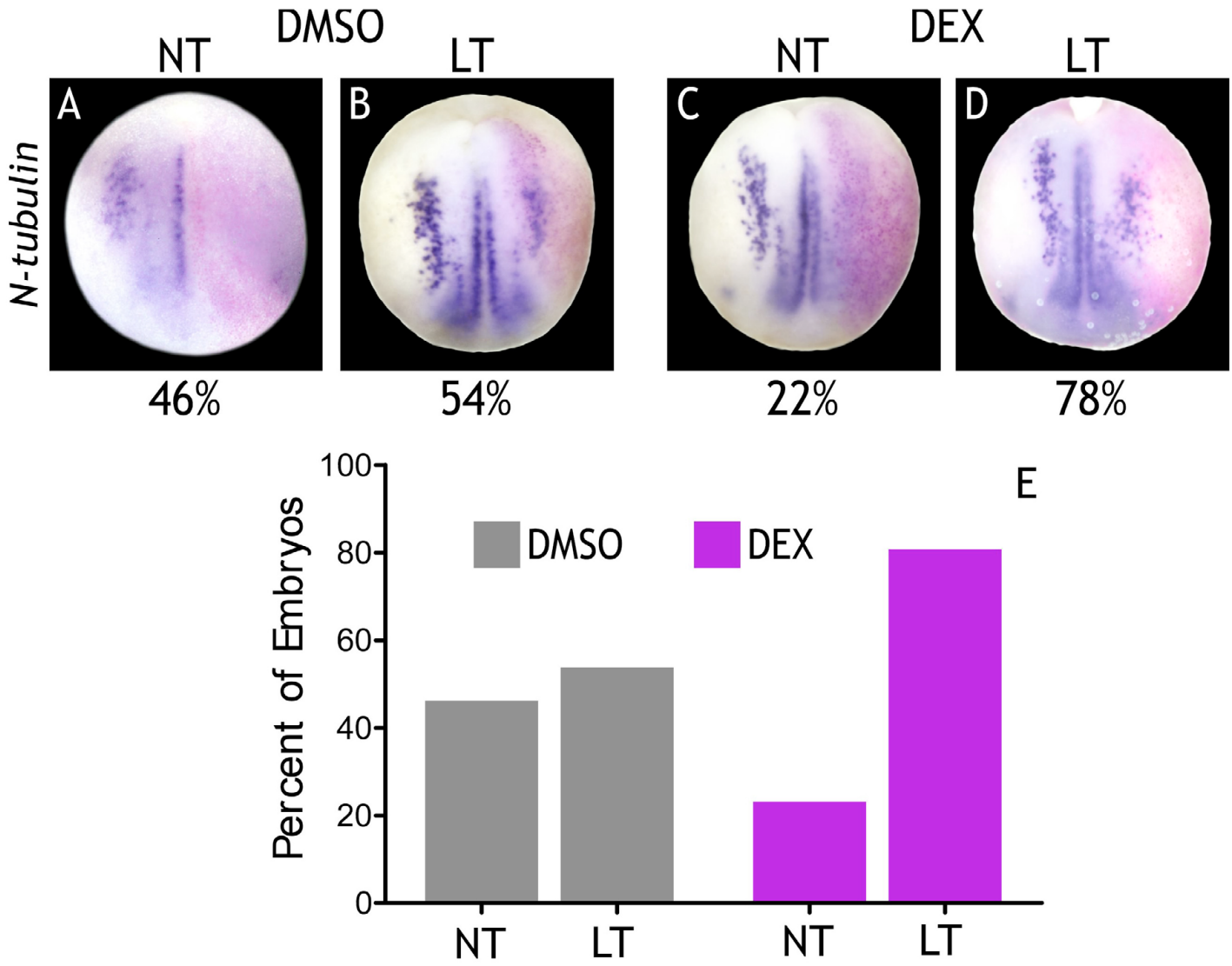

Fig. S16. ERF gain-of-function partially rescues *N-tubulin* expression in RARγ-MO embryos. All embryos were injected unilaterally with 3.75 ng *Rarγ1* MO + 3.75 *Rarγ2* MO + 0.1 ng *hGR-Erf* ($S^{246,251}\rightarrow A^{246,251}$) mRNA at the two- or four-cell stage, then treated with 10 μM dexamethasone (DEX) or 0.1% DMSO vehicle at stage 11. The injected side is indicated by the magenta *β-gal* mRNA lineage tracer. (**A**,**B**) Embryos treated with DMSO exhibited no tubulin (NT) or low tubulin (LT) of *N-tubulin* in 46% and 54% of embryos, respectively. (**C**,**D**) Embryos treated with dexamethasone exhibited no tubulin (NT) or low tubulin (LT) of *N-tubulin* in 23% and 81% of embryos, respectively. All embryos are shown in dorsal view with anterior at the bottom, at stage 13/13.5. (**E**) Scoring of embryos.

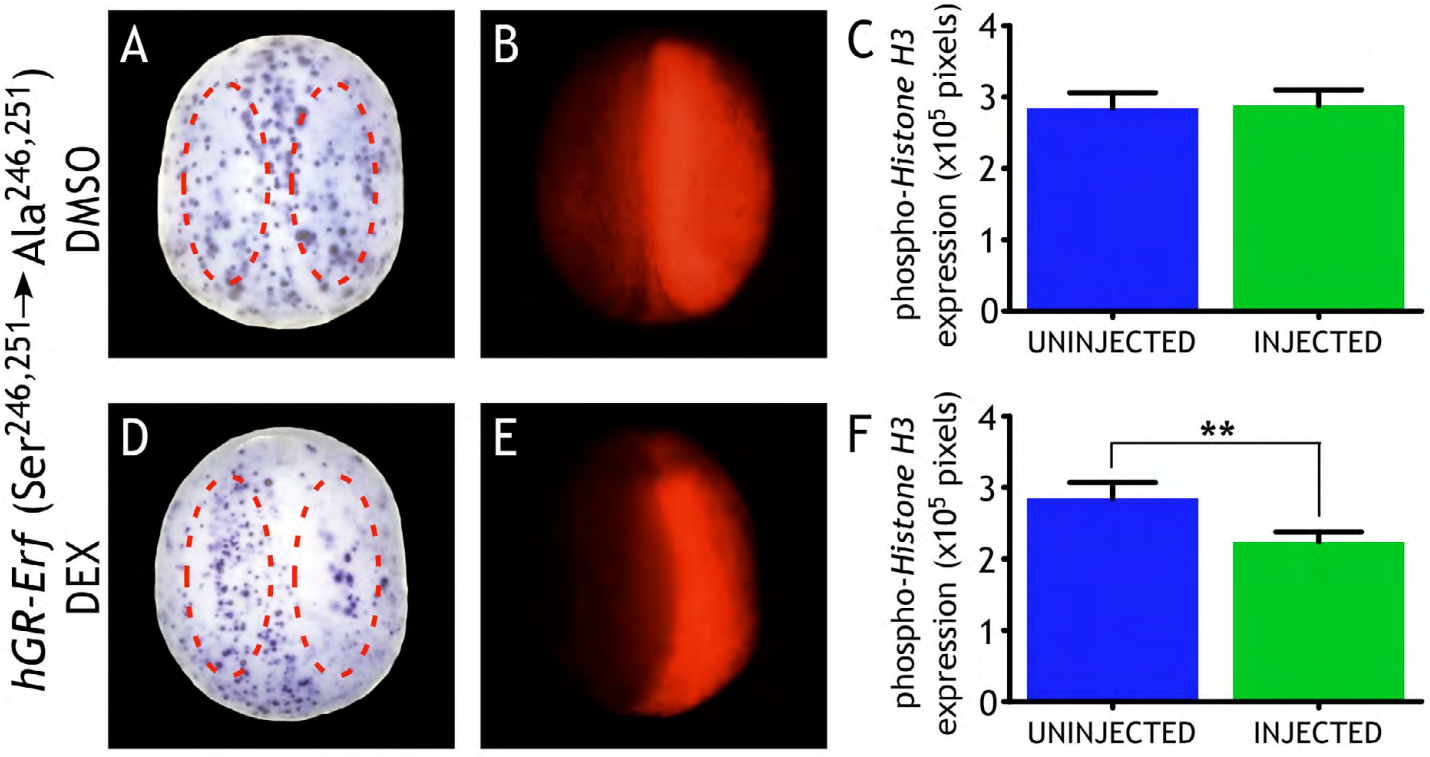

Fig. S17. ERF gain of function decreases proliferation in the neural plate. Embryos were injected unilaterally at the 2- or 4-cell stage, then treated with 10 µM dexamethasone (DEX) or 0.1% DMSO vehicle at stage 11. The injected side is indicated by the red fluorescent lineage tracer. (**A**,**B**,**D**,**E**) Representative photographs in bright field (A,D) and fluorescence (B,E) are shown. (**C**,**F**) Quantitation of phospho-*Histone H3* staining for all embryos in the experiment. Embryos are shown in dorsal view at stage 14; anterior is at the bottom. (A-C) DMSO-treated embryos injected with 0.1 ng *hGR-Erf* ($S^{246,251}\rightarrow A^{246,251}$) mRNA showed no significant difference in the number of phospho-*Histone H3* nuclei on the injected versus the uninjected side (n=30; P=0.758). (D-F) Dexamethasone-treated embryos injected with 0.1 ng *hGR-Erf* ($S^{246,251}\rightarrow A^{246,251}$) mRNA showed a decreased number of phospho-*Histone H3* nuclei on the injected versus the uninjected side (n=37; P=0.0028).

Table S1. Morpholinos

MO	**Type**	**Sequence (5′→3′)**
Rarγ1	AUG	GCT GTT TGC CAT TGC CTT GTT CTA
Rarγ2	AUG	TTC CAT GCA GTC ATA CAT TTT GGG
Rarα1:	AUG	GCT CCA AAC GCA CTT CTA CTC CCT C
Rarα2.1:	AUG	CTG AAA TCC AAA CTG ACC ATA GAG T
Rarα2.2:	AUG	ATC CAA AGG AAG GTG AGT GTG TGT G
Rarα (D1)	Splice	GGG TAA CAC TTA CCT TGC AAC CTT C
Rarα (D2)	Splice	GCG CCC GTT ACT CAC ATT CTT TAG A
Raldh2	AUG	TCT CTA TTT TAC TGG AAG TCA TGT C
Cyp26a1	AUG	TAG TGA GCA GAG TAT ACA GAT CCA T
Etv3l	AUG	CCT TCT CTT CTT GCT TAG TAA CAT C
Etv3	AUG	GTT TCC TTC TTG CTG ACG GGA TCG A
Erf #1	AUG	CCA CTA GCG CTG CTC TCC CCT CGG T
Erf #2	AUG	GGT CTG TGC TGC TTC TCC TCC TCC A

Table S2. Probes with T7 adapters

Primer	**Sequence (5′→3′)**
F (*Geminin*):	TAC CAA CAA GAA GCA GAG ATT GGA
R (*Geminin*):	taa tac gac tca cta tag ggA TTC TGA TCT GAA TTA GAG GGC CG
F (*Foxd4l1*):	ATG CAG GAC TTT CTG ATG AGG A
R (*Foxd4l1*):	taa tac gac tca cta tag ggT AAG CAC AGC TGG GAG AAG G
F (*Neogenin*):	AGC CCG ACT TCA CTG GAT CA
R (*Neogenin*):	taa tac gac tca cta tag ggC TGT GGT TAT GGC ATT TAG ATC
F (*Sox3*):	GTT GGA CAC CGA CAT CAA GAG
R (*Sox3*):	taa tac gac tca cta tag ggG TAC CGT GCC ATT GAC TCC A
F (*Zic1*):	GTG ACG ACT TTC GGT TCC TC
R (*Zic1*):	taa tac gac tca cta tag ggG TGA TTG GAC GTG TGA TGT ACT G
F (*Zic3*):	ACA ATG CTA TTA GAT GGA GGA CCG
R (*Zic3*):	taa tac gac tca cta tag ggT GTT GTT AGT CTG ATG TGT TGC TG

Table S3. Probe plasmids

Gene	Restriction enzyme	Polymerase
Dl1	*Xho*I	T7
Myt1	*Cla*I	T7
Ngnr1	*Bam*HI	T3
Zic2	*Bam*HI	SP6

Table S4. QPCR

Primer	Sequence (5′→3′)
F (*Etv3*)	GGA AGT GGG ATT AAT AAG GCG G
R (*Etv3*)	CCG TCA GCA AGA AGG AAA CAT G
F (*Etv3l*)	GCG ACC AAT TCC TAC GTG TG
R (*Etv3l*)	GCT GTT CTT CAG GTT CAA ACT TCC
F (*Erf*)	TTC GGA AAT GCA AAC CGC AG
R (*Erf*)	GGT AAA GCG TTT GCC TTT GGT
F (*HoxA1*)	AAG TTT GTG GTT CTC CTG CC
R (*HoxA1*)	TTT GTG GTG AAG TTG GTC CTG
F (*Histone H4*)	GAT AAC ATC CAG GGC ATC AC
R (*Histone H4*)	TAA CCT CCG AAT CCG TAC AG

Table S5. Cloning pCDG1-FLAG-*Erf-hGR*$^{512\text{-}777}$

Primer	Sequence (5′→3′)
A	CAG ATA CCA TGG ATT ATA AAG ATG ATG ATG ATA AGC TTA TGA AAA CCC CGG CAG AG
B	GGA TTT TCA GAT CTG GAA TCG CGG TTT TCC AGG
C	CCG CGA TTC CAG ATC TGA AAA TCC TGG TAA CAA AAC AAT AG
D	ACT AGT GGA TCC TTA CTA TCA CTT TTG ATG AAA CAG AAG TTT TTT G

Table S6. Cloning pCDG1-FLAG-Erf-hGR$^{512-777}$ mutants

Primer	Sequence (5′→3′)
A	CAG ATA CCA TGG ATT ATA AAG ATG ATG ATG ATA AGC TTA TGA AAA CCC CGG CAG AG
B (Ala^{237}, Ala^{242})	**TGC** CAC TGG GAA TGG **TGC** GAG AGG CTC TGG CAC CCG
B (Glu^{237}, Glu^{242})	**TTC** CAC TGG GAA TGG **TTC** GAG AGG CTC TGG CAC CCG
C (Ala^{237}, Ala^{242})	**GCA** CCA TTC CCA GTG **GCA** CCC ATG GGT GCA CCA GC
C (Glu^{237}, Glu^{242})	**GAA** CCA TTC CCA GTG **GAA** CCC ATG GGT GCA CCA GC
D	ACT AGT GGA TCC TTA CTA TCA CTT TTG ATG AAA CAG AAG TTT TTT G